COOLING CITIES FOR HEALTH THROUGH URBAN GREEN INFRASTRUCTURE: A HEALTH IMPACT ASSESSMENT FOR EUROPEAN CITIES

Tamara Iungman[1,2,3], Marta Cirach[1,2,3], Federica Marando[4], Evelise Pereira-Barboza[1,2,3], Sasha Khomenko[1,2,3], Pierre Masselot[5], Marcos Quijal-Zamorano[1,2], Natalie Mueller[1,2,3], Antonio Gasparrini[5,6,7], José Urquiza[1,2,3], Mehdi Heris[8], Meelan Thondoo[1,9], Mark Nieuwenhuijsen[1,2,3]

1 Institute for Global Health (ISGlobal), Barcelona, Spain

2 Department of Experimental and Health Sciences, Universitat Pompeu Fabra, Barcelona, Spain

3 CIBER Epidemiología y Salud Pública (CIBERESP), Madrid, Spain

4 European Commission – Joint Research Centre, Ispra, Italy

5 Department of Public Health, Environments and Society, London School of Hygiene and Tropical Medicine (LSHTM), London, UK

6 Centre on Climate Change and Planetary Health, London School of Hygiene & Tropical Medicine (LSHTM), London, UK

7 Centre for Statistical Methodology, London School of Hygiene & Tropical Medicine (LSHTM), London, UK

8 Hunter College City University of New York

9 MRC Epidemiology Unit, University of Cambridge School of Clinical Medicine, Cambridge, UK

Correspondence to:

Prof. Mark Nieuwenhuijsen,

ISGlobal, 08003, Barcelona, Spain

mark.nieuwenhuijsen@isglobal.org

Research in context

Evidence before this study

We conducted two different literature searches in the PubMed, Scopus and Google Scholar databases, without language or publication date restrictions. The first one searched for estimates of the impacts of the urban heat island on health while the second one searched for health impacts that could be avoided by increasing the urban green infrastructure. For both cases we only considered studies carried out in European cities. Our search revealed that there are only a few studies conducted in this realm, which are only restricted to a small number of European cities. We found a large body of evidence based on time-series studies, studying the impacts of suboptimal temperatures on mortality, but only a couple of studies focused on the mortality fraction attributable to the urban heat island, all of them occurring during heat-wave events. We found only a few studies that assessed the potential preventable mortality burden of urban green interventions, however, all studies focused on extreme heat episodes.

Added value of this study

To our knowledge, this is the first study to estimate the mortality burden attributable to the urban heat island and the mortality burden that could be prevented by increasing the tree cover in European cities. The added value of the study is mainly constituted by the extent (covering 93 European cities) and the resolution (250 m cell size) of the health impact assessment of urban heat islands, which is unprecedented. The spatially explicit analysis of urban heat exposure and its interaction with urban vegetation informs future realistic city-specific scenarios that can help mitigate adverse heat-related health impacts.

Implication of all available evidence

Our results showed that considerable mortality impacts can be attributed to the urban heat island in European cities. Most importantly, these impacts could be considerably reduced by increasing the tree cover and thereby providing cooling in urban environments. This evidence together with the spatial information of the areas that would benefit the most from increasing the tree cover is valuable to policymakers in view of targeted green interventions to maximize population health benefits while promoting more sustainable and climate-resilient cities.

ABSTRACT

BACKGROUND: High ambient temperatures are associated with many health effects including premature mortality. Given the current warming trend due to climate change and the global built environment expansion, the intensification of urban heat islands (UHI) is expected, accompanied by adverse impacts on population health. Urban green infrastructure can reduce local temperatures. We aimed to estimate the mortality burden that could be attributed to the UHI and the mortality burden that would be prevented by increasing the urban tree cover (TC) in 93 European cities.

METHODS: We conducted a quantitative health impact assessment (HIA) for the summer (June-August) of 2015 to estimate the impact of the UHI, on all-cause mortality for adult residents (≥ 20 years old) in 93 European cities. In addition, we estimated the temperature reduction resulting by increasing the TC to 30% for each city and estimated the number of deaths that could be potentially prevented as a result with the aim of providing decision-makers with usable evidence to promote greener cities. We performed all analyses at a high-resolution grid-cell level (250m x 250m).

FINDINGS: The population-weighted-city-average UHI from June to August was 1.5°C (city range 0.5°C - 3.0°C). Overall, 6,700 (95% CI 5,254 - 8,162) premature deaths could be attributable to the UHI (ie, 4.3%, city range 0.0%-14.8% of summer mortality, 1.8%, city range 0.0%–2.8% of annual mortality). Increasing the TC up to 30% at 250m resolution resulted in an average city cooling of 0.4ºC (city range 0.0ºC-1.3ºC). We estimated that 2,644 (95% CI 2,445-2,824) premature deaths (ie, 1.8%, city range 0.0%-10.8% of summer mortality, 0.4%, city range 0.0%–2.0% of annual mortality) could be prevented by increasing the average TC in cities to 30%.

INTERPRETATION: Our results showed the impacts on mortality of the UHI and highlight the health benefits of green infrastructure to cool urban environments, while promoting more sustainable and climate-resilient cities.

Funding. GoGreenRoutes, Spanish Ministry of Science and Innovation, Internal ISGlobal fund, Medical Research Council-UK, European Union's Horizon 2020 Project Exhaustion.

Keywords: urban heat island, urban green infrastructure, tree cover, cooling, mortality, health impact assessment

INTRODUCTION

Many epidemiological studies have provided evidence on how extreme temperature affects human health and mortality. Exposure to high ambient temperatures has been associated with premature mortality (1,2), cardiorespiratory morbidity (3,4), hospital admissions (5) and children´s mortality and hospitalization (6). Temperature and mortality are related not only during extreme hot temperature events, such as heat waves, but also under moderately warm temperatures (2,7). Small changes at mild or moderate temperatures may occur more frequently, and therefore can have significant health impacts (2,8,9).

The urban heat island (UHI) phenomenon refers to the temperature difference between the city and its surrounding areas and it is considered as one of the most striking climatic manifestations of urbanization (10). The UHI originates from the anthropogenic modification of natural landscapes such as changes in the pattern of vegetation and water bodies through fragmentation and conversion into impermeable surfaces (11). The increased absorption and trapping of solar radiation in built-up urban fabrics, increasing population density and the absence of green areas are the main factors that have been associated with the UHI formation (12). The UHI may intensify the impact on health of high temperatures, increasing health risks for the most vulnerable populations (13). A study in the West Midlands, UK estimated that the UHI contributed around 50% of the total heat-related mortality during the 2003 heatwave (14). Another study in Ho Chi Minh City, Vietnam, compared the heat related mortality between the central and outer districts and estimated that the attributable fraction resulting from the UHI was 0.42% (15).

Previous studies have reported a nonlinear association between temperature and mortality, characterized by U- or J- shaped association (1–3). These associations vary dramatically between populations due to differences in susceptibility, age distribution, access to resources, adaptability and local public policies (e.g. extreme heat warning systems, healthcare system preparedness, etc)(1). The modelling of such complex patterns requires a sophisticated statistical approach and the collection of large historical data (2). Masselot et al (forthcoming) have provided mortality risk estimates for 801 European cities by age group accounting for a large list of city-level socio-economic, climatic, and environmental characteristics (16), enabling the performance of Health Impact Assessment (HIA) studies for estimating the impacts of potential temperature variations, for instance, using a comparative risk assessment (CRA) approach.

The CRA HIA approach evaluates the potential changes on the population health that would result from shifting baseline exposure levels to an alternative, counterfactual exposure level scenario (17). This approach serves as a decision-making framework with robust and usable evidence on the implication of health-promoting scenarios that could be achieved through specific urban planning strategies (18). The CRA HIA approach can be applied at high spatial resolution level, and therefore, can capture spatial variability, which carry important environmental justice and health equity implications.

There are a few known planning and design strategies to mitigate urban heat: (1) Introducing green roofs or facades (19–22); (2) enhancing the reflective properties (ie, albedo) of buildings by using light colours for roof and wall surfaces (20,23); (3) replacing impervious surfaces with permeable or vegetated areas (24–26); and (4) increasing the tree cover (TC) (27–30). Urban trees may offer an important opportunity to mitigate high temperatures while constituting a relatively simple and cost-effective solution (28). Marando et al (2021) have estimated the cooling capacity of trees in more than 600 European cities (27). The authors simulated the temperature difference between a baseline and a no-vegetation scenario, extrapolating the role of trees in mitigating UHI in different urban contexts. Urban trees were found to cool European cities by about 1.07 °C on average, and up to 2.9 °C (27). A recent evidence-based guideline has recommended a 30% TC goal per neighbourhood for cooling, improving the microclimate, mitigating air and noise pollution and improving mental and physical health (31), and many cities have already set a 30% of TC as a target (32–36). Furthermore, previous epidemiological studies have reported health benefits of exposure to 30% or more TC including lower odds of incident psychological distress (37) and non-communicable diseases (NCD) such as diabetes, hypertension and cardiovascular disease (CVD) (38).

Given the ongoing global warming and the urban sprawl and development of natural lands , the intensification of UHIs is expected (6,39,40). While the benefits of global mitigation strategies have been well discussed, the health benefits of improving local climate through improving the urban planning in cities are still unknown. Furthermore, compared with global efforts, some local actions to improve urban climate offer the advantages of being politically easier to implement and of having short-term benefits (41).

We conducted a quantitative HIA in 93 European cities to estimate the annual mortality burden that could be attributed to the UHI. We also estimated the mortality burden that could be prevented if reduction in temperature is achieved by increasing the TC to 30%, following the target already adopted by many cities. Our ultimate goal is to inform local policy and decision-makers on the benefits of strategically integrating urban green infrastructure (UGI) into urban planning in order to promote more sustainable, resilient and healthy urban environments and contribute to climate change adaptation and mitigation.

METHODS

Cities selection

European cities and their boundaries were defined from the Urban Audit 2018 dataset of Eurostat (42). This database includes data for all European cities with more than 50,000 inhabitants, also including greater cities (Supplement A). We selected the cities based on the Urban Climate (UrbClim) model temperature data availability (43). The dataset includes 100 cities, six of which were not included in the Urban Audit dataset (ie, Belgrade, Novi Sad, Podgorica, Sarajevo, Skopje and Tirana). We also excluded Reykjavic, Iceland, due to lack of exposure-response function (ERF), therefore analysed the remaining 93 cities. Given that the City of London is more of an economic centre rather than a residential place (ie, with only 8,200 inhabitants living by 2015), we decided to include London Greater City instead (Supplement A), hereafter referred to as city and increase the coverage in terms of city size and population.

Population data

We retrieved demographic data following the procedure well described by previous HIA studies for European cities (44–46). Briefly, we retrieved total population counts for each city from the Global Human Settlement Layer (GHSL) for 2015 (47), which was the latest available population layer in a high resolution (ie, 250 m × 250 m). We excluded from the baseline GHSL dataset the non-residential areas (ie, industrial zones, port areas and water bodies, airports, parks) to better represent population distribution, based on land use data from European Urban Atlas 2012 (48). We reallocated the population from the removed grid cells among the dataset according to the GHSL population distribution to maintain the total city population counts (Supplement B). We retrieved the population age distribution for 2015 from Eurostat at the Nomenclature of Territorial Units for Statistics (NUTS) 3 level (42)). We calculated the proportion of population in each 5- year age group by NUTS3 and estimated the population distribution by age group. We aggregated the groups as 20-44, 45-64, 65-74, 75-84 and 85 years and older to fit them with ERFs (Supplement B).

All-cause mortality

We retrieved weekly all-cause mortality counts by age group for 2015 from Eurostat (42), available for 81 cities at NUTS3 level. We estimated the daily mortality rates per age group per city assuming the same distribution as the NUTS3 and a homogeneous distribution of deaths over the same week and applied the rates to each grid cell.

For cities without weekly deaths counts available (n = 12) (Supplementary Table 1), we retrieved annual city-specific all-cause mortality counts for 2015 from Eurostat (42). We estimated the mortality rates per age group and applied the rates to each grid cell. We retrieved monthly country mortality counts (42) and estimated the proportion of deaths per month. We assumed a homogeneous distribution of deaths over the same month and estimated the daily deaths per grid cell.

The daily mortality counts estimated correlated strongly between the two methods for the 81 cities for which data was available (Pearson correlation=0.98), however with an overestimation of the annual city-specific mortality counts (17%). Therefore, we calibrated it (Supplement B).

Baseline exposure to heat

We defined the baseline exposure scenario as the daily mean temperature for the corresponding baseline 2015 TC of each city. We retrieved daily mean temperature from the Urban Climate (UrbClim) model for 93 cities at 100m x 100m resolution (43). The model combines large-scale meteorological data on surface, sea, precipitation, soil, and vertical profile, and a description of the terrain that includes land use, vegetation (Normalized Difference Vegetation Index, NDVI), and soil sealing. Temperature series were created by averaging the 100m grid cells with centroids within the spatial boundaries of each 250m grid cell.

Health Impact Assessment (HIA)

We conducted a quantitative HIA at 250 m by 250 m grid cell level for the year 2015, for the adult population > 20 years old residing in the 93 cities (n = 57,896,852) based on the GHSL residential population (47). We considered the summer period from June 1st to August 31^{st}, based on previous seasonality studies on temperature-attributable mortality (49). Year 2015 was found typical of the current climate temperature-wise (Supplement C). We followed a quantitative HIA approach based on CRA methodology (44–46). We conducted two main analyses. The first analysis estimated the impact of the exposure to the UHI effect on mortality, therefore, we compared the baseline temperature exposure with a counterfactual exposure, although non-realistic, without UHI. The second analysis estimated the mortality impact of increasing the TC to 30%, as recommended, and the subsequent temperature reductions.

We retrieved city and age group-specific exposure-response functions (ERFs) from Masselot et al (16). We estimated the daily baseline temperature exposure levels and we calculated the Population Attributable Fraction (PAF) for each daily mean and age group. We estimated the attributable premature mortality burden combining the PAF and the daily all-cause mortality

(Supplement C). We repeated the same procedure for each of the counterfactual scenarios and we calculated the difference with the baseline scenario. The obtained result is the premature mortality burden attributed to shifting baseline exposure levels to the specific counterfactual exposure level scenario (ie, UHI effect or 30% TC) (Figure S1).

We added up the results by city and estimated the preventable age-standardized mortality per 100,000 population, based on European Standard Population (ESP) (50) and the percentage of preventable annual and summer all-cause deaths. Additionally, we calculated the Years of Life Lost (YLL) due to the premature deaths (Supplement C).

We performed the analysis considering the sources of uncertainty. The parameters considered were: the ERFs, the UrbClim temperature data error, the temperature adjustment model error, the UHI data error and the cooling model error, accordingly. We constructed the uncertainty distribution for each parameter and estimated the point estimates and 95% confidence intervals performing 500 Monte Carlo iterations by sampling from the built uncertainty range, considering all the parameters uncertainties at the same time in order to have the cumulative uncertainty.

Finally, we ran Pearson correlations assessing the association between the outcomes from the UHI scenario and the 30% TC scenario.

Exposure response functions (ERFs)

We retrieved the ERFs quantifying the association between temperature exposure and all-causes mortality by city and age group (ie, 20-44, 45-64, 65-74, 75-84 and 85 years and older) from Masselot et al (forthcoming) (16), which considers a comprehensive list of city-level characteristics making the ERFs the best evidence available in the literature.

Given that the risk estimates were built under the ERA5-LAND temperature dataset with a resolution of approximately 9 km, therefore covering rural areas, it was expected that the ERF temperature range was lower than the UrbClim temperature range. For that reason, we applied a city-specific correction to the UrbClim dataset (Supplement D).

Counterfactual levels of exposure to heat

Urban Heat Island. We retrieved the mean day-time UHI and mean night-time UHI data at 100 m x 100 m resolution for 2015 summer season (ie, June - August) from the Copernicus UrbClim model application (43). The UHI is estimated as the difference between the mean rural temperature (ie, represented by the rural classes of CORINE) and each of the urban grid cells

(43). We estimated the 250m grid cell 24-h daily mean UHI by averaging the day and night UHI 100 m grid cells with centroids within the spatial boundaries of each 250 m grid cell (Supplement E, a). In spite of the known differences between day-time and night-time UHI we averaged them given that the available ERFs consider 24 hours of exposure to a daily mean temperature. For the grids with negative values we considered a null UHI (Supplement E, a).

TC 30%. We estimated the decrease in temperature, ie cooling effect, as the result of increasing the TC up to 30% at a grid cell level. The Copernicus HRL Forest defines TC as the vertical projection of tree crowns to a horizontal earth's surface (51). For each city, we analyzed the feasibility of achieving this counterfactual by estimating the percentage of open space where potentially trees could be planted according to the corresponding land use. On average, cities presented a mean difference between the open space and the 30% target at a grid-cell level of 2.9%, ranging from 0.1% to 7.7%, indicating the reasonable target for European cities (Supplement E,b).

As an additional analysis, we set a more attainable scenario of 25% TC, based also on previous studies´ translations of the WHO recommendation on access to green spaces (52,53); and a more ambitious of 40% TC, based on a previous research suggesting a 40% TC for having significantly reduced daytime air temperature (29).

We followed the Marando et al (2021) and Heris et al´s (2021) approach (27,54), which determined the best fitted models through Machine Learning techniques were linear regressions. Briefly, (i) first, we retrieved Landsat-8 Images (30m x 30m resolution) (55) and estimated the median Land Surface Temperature (LST) (June-August, 2015) for each grid cell. (ii) Then, for each city, we developed a linear regression model with an ordinary least square algorithm trained by the LST (°C) dataset, the TC (retrieved from Copernicus at 100m x 100m resolution) (51) (Supplement D, b) and the amount of water evaporated from trees at 500m x 500m resolution (Etree, mm day−1), which is the sum of transpiration and vaporization of intercepted rainfall from vegetation (from PML V2 evapotranspiration product, based on the Penman-Monteith-Leuning canopy conductance model, (56,57)) to estimate the impact of trees on surface temperature reduction at grid-cell level (Eq. 1).

Eq. (1) $$\mathbf{LST = \beta_{0e4} + \beta_{1e4}TC + \beta_{2e4}Etree}$$

(iii) After that, we built a second ordinary least squares model, trained with an air temperature dataset for predicting the maximum air temperature (Tair, °C) as a function of LST and latitude (Eq. 2). The existing network of weather stations in Europe has insufficient coverage and therefore cannot be used for the aforementioned purposes, so we used a US air temperature dataset (Supplement E, b).

$$\textbf{Eq. (2)} \qquad \mathbf{Tair = \beta_{0e5} + \beta_{1e5}LST + \beta_{2e5}Latitude}$$

We validated the model through a linear regression between the predicted values and the UrbClim values with an adjusted R2 equal to 0.66 and a RMSE% of 2.03 (Supplement E, b).

iv) In order to estimate the LST corresponding to TC equal to 30%, 40% and 25%, we estimated the city-average Etree considering the grid cells with: (1) TC=28-32% (Etree30) and, (2) TC=38-44% (Etree40), (3) TC=23-27% (Etree25), respectively. We considered an interval plus-minus 2º for avoiding low counts.

v) Finally, we set the counterfactuals as 30% (main analysis), 40% and 25% TC (additional analyses) and estimated the respective LSTs by replacing in Eq.2 with the corresponding TC and Etree. We estimated the Tair with the obtained LST with the Eq. 2 and we calculated the difference between the baseline Tair and the counterfactual Tair. This difference is the cooling we would obtain if increasing the TC from baseline to 30%, 40% and 25%, accordingly, at grid-cell level and is the temperature reduction we used as our counterfactual in the HIA. All of the grids with negative cooling values were set to Null (ie, 16%) (Supplement E,b). In addition, 3.6% of the grid cells, covering 3.4% of the total population, were excluded from the analysis due to missing values of any of the parameters required for running the model. The error of the model has been estimated by calculating the propagated error of the two regressions, for each city, as described by Marando et al (2021) (27) (Supplement E, b). The city-average R squared was of 0.41 (city range 0.07 – 0.79).

Sensitivity analyses

We conducted sensitivity analyses to assess the effects of changes in the HIA input variables on the magnitude of our mortality estimations. We evaluated for both HIA scenarios (i.e. UHI effect and 30% TC) the effects of using Martinez-Solanas et al (2021) ERFs, available for 147 European regions (NUTS2) covering 66 cities (58). For the UHI scenario, we assessed the effects of using the adjusted and the non-adjusted annual city-specific mortality datasets, the impact of using the grid-average summer UHI as well as the city-average summer UHI. For the 30% TC scenario, we assessed the effects of using the city-average cooling. In addition, we conducted a sensitivity analysis of the cooling model by changing the Etree30 estimation. We ran linear regression by city between the TC and the Etree and predicted the Etree when TC was 30%. A second approach was to run the regressions between the TC and the Etree grouping by biome, given that the Etree is associated with the vegetation and climate of the region (56,59). In this way, we increased the counts and avoided poor adjustments. We evaluated the effects on the city-average cooling as well as on the 30% TC (Supplement F).

Uncertainty analysis

In order to understand the uncertainty contribution of each parameter in our confidence interval, we performed an uncertainty analysis for 6 selected cities for both HIA scenarios (UHI effect and 30% TC). For this, we ran 500 Monte Carlo simulations considering each of the parameter’s uncertainty separately. We selected the cities in order to have two cities with high mortality impacts (ie, Barcelona and Budapest), two cities with moderate mortality impacts (ie, Munich and Lodz) and two cities with low mortality impacts (ie, Riga and Rotterdam) (Supplement G).

Cooling effort Index

We created an indicator of the TC increment efforts needed to cool down cities, which is the ratio between the cooling effect of TC at 30% and the average increase in TC to reach the target of 30%, hereafter refer to as *Cooling Effort Index*. It can be interpreted as the cooling we could obtain per 1% of TC increment.

RESULTS

Overall, 57,896,852 inhabitants over 20 years old resided in the 93 studied cities in 2015. City population counts ranged from 95,242 (Tartu, Estonia) to 8,011,216 (London Greater City, UK), with a median population size of 624,495 inhabitants. In total 555,215 deaths from all causes were reported for the same year with 23.1% (n=128,269) having occurred from June to August. Overall, summer average temperatures ranged between 14.2°C in Glasgow, UK, and 29.7°C in Sevilla, Spain, with average maximum temperatures ranging between 22.7°C in Tallín, Estonia, and 36.8°C in Sevilla, Spain. The population-weighted-city- average daily UHI from June to August was 1.5°C (city range 0.5°C -3.0°C) (Figure 1) with maximum grid-cell values reaching 4.1°C in Cluj-Napoca, Romania (Supplementary Table 1).

The city-average TC was 14.9% (city range 2.1%-34.6%), whereas the grid-cell-population-weighted-average was 10.9% (city range 1.8%-29.9%). We estimated that increasing the TC up to 30% at 250m resolution would result in an average city cooling of 0.4°C (city range 0.0°C - 1.3°C) (Figure 1) with maximum grid-cell values of 5.9ºC (Supplementary Table 1). Increasing the TC to 30% at a grid-cell level would lead to a city-average increase of 17.7% (city range 3.8%-28.8%) (Supplementary Table 1).

Across all examined cities, almost 75% and 20% of the total population (57,089,394 and 14,491,628 inhabitants) lived in areas with an average-summer UHI greater than 1ºC and 2ºC, respectively. Overall, 6,700 (95% CI 5,254 - 8,162) premature deaths could be attributed to the UHI during the summer months (ie, 4.3%, city range 0.0%-14.8% of summer mortality, 1.8%, city range 0.0%–2.8% of annual mortality) and 2,644 (95% CI 2,444-2,824) premature deaths could be prevented by increasing the TC up to 30% (ie, 1.8%, city range 0.0%-10.8% of summer mortality, 0.4%, city range 0.0%–2.0% of annual mortality) (Table 1, Figure 2). This corresponds, on average, to 39.5% of the deaths attributable to the UHI.

A great variability in the attributable mortality burden was observed among the cities. The UHI was associated with a range of 0 (Göteborg, Sweden) and 32 (Cluj-Napoca, Romania) premature deaths per 100,000 age-standardized population, with an average of 10 deaths per 100,000 age-standardized population (Table 2, Figure 2). The increase in the TC to 30% could prevent between 0 (Oslo, Norway) and 22 (Palma de Mallorca, Spain) premature deaths per 100,000 age-standardized population (Table 3, Figure 2).

Overall, cities with the highest mortality rates attributable to the UHI were in Southern and Eastern Europe, particularly in Spain, Italy, Hungary, Croatia and Romania. While cities with the lower UHI attributable mortality rates were mainly located in Northern Europe including Sweden, Estonia, UK, and northern France (Table 2, Figure 2). A similar pattern was observed for the mortality rates that could be prevented by increasing the TC (Table 3, Figure 2). Indeed, the number of deaths attributable to the UHI and the number of preventable deaths for increasing the TC to 30% were strongly linearly correlated (r=0.89), as well as the attributable mortality rates (r=0.75), the percentage of annual attributable mortality (r=0.73) and the attributable YLL (r=0.89) (Supplement C).

For the UHI scenario, the sensitivity analyses indicated that the largest variations in the final estimates were due to the use of the non-adjusted city-specific annual mortality dataset (+20%), followed by the use of the average city UHI (-18%), followed by the change in the ERF. For the 66 cities covered, the use of the Martínez Solanas ERF represented a 17% decrease in the impacts on the estimated preventable mortality burden. The use of the adjusted city-specific annual mortality dataset and the average-summer UHI by grid resulted in slightly higher estimates (ie, +3% and +2%, accordingly) (Table 1).

We observed great changes in the mortality burden estimations under alternative counterfactual scenarios. The more ambitious TC counterfactual scenario equal to 40% would lead to a 41% increase in the mortality burden with an average city cooling of 0.5°C, whereas the more attainable TC counterfactual scenario equal to 25% would lead to a 21% decrease in the mortality burden with an average city cooling of 0.3°C. The use of Martinez-Solanas et al (2021) ERF supposed a decrease of 21% followed by the use of the average cooling by city (-19%) (Table 1). Finally, the changes in the cooling estimations resulted in minor differences in the estimates (+1% and +3% for using linear regressions by city and by biome, respectively) (Table 1). Taken as a whole, the sensitivity analyses showed high robustness of our results, as the observed changes correlated strongly with our main estimations (Supplement F).

Uncertainty analysis of the UHI scenario showed that the UHI was the primary contribution of uncertainty, followed by the baseline temperature, the ERF and the temperature adjustment to ERA5. For the 30% TC scenario, the baseline temperature was the primary source of uncertainty, followed by the ERF, the cooling model and finally, the temperature adjustment to ERA5. (Supplement G).

Cities with higher *Cooling Effort Index* were mainly located in Northern Europe (ie, Oslo, Edinburgh, Göteborg, Tallin) but were also geographically-dispersed and included Sofía, Liège, Krakow, Graz, Nantes and some cities in northern Italy (ie, Torino, Bologna, Genova). Whereas cities with lower *Cooling Effort Index* were mostly located in the Southern Europe (ie. Athens, Thessaloniki, Bari, Varna, Valencia, Porto), they were also dispersed across Central Europe (ie, Zurich, Padova, Milano, Leipzig, Munich) (Figure 1).

DISCUSSION

This is the first study to estimate the mortality burden attributable to the UHI and the mortality burden that could be prevented by increasing the TC in European cities. Our results show that a large number of deaths (6,700, 95% CI 5,254 - 8,162) could be attributed each summer to the UHI and that 39.5% of these deaths can be avoided by increasing the TC in cities to 30%.

Our results align with prior studies estimating the cooling obtained from UGI strategies. Sailor et al (2003) estimated that a 10% increase in the TC, could reduce urban temperatures in Philadelphia, U.S., by 0.22°C (60), while another study for New York City, U.S, estimated a potential 0.6°C reduction at 3 p.m. if 31% of the city area were covered with trees and green roofs (22). In addition, a recent systematic review on cooling modelling showed that street trees can reduce urban air temperature on average 0.3°C per each 10% TC increase (61). We estimated that a city-average increase of 17.7% (ie, for reaching TC=30%) would cool European cities by 0.4°C on average (city range 0.0°C -1.3°C). Nevertheless, according to Marando et al (2021), temperatures could be reduced by 1°C on average in an European Functional Urban Area (FUA) with a TC of 16% (27). Despite of having used a similar methodology, our estimates are notably lower. The differences obtained can probably be explained by the area of scope of the study. While we developed the model at a city level, Marando et al (2021) did it at a FUA level, which is constituted by a core city and its commuting zone, often including greener areas (ie, peri-urban forests). This has two main consequences, particularly regarding the Etree layer. First, since this layer has a rather coarse spatial resolution (500m x 500m) it might not well capture spatial heterogeneity at city level, especially in the case of scattered trees (27). Second, a different transpiration rate of trees in highly urbanized settings, compared to peri-urban areas, has been previously reported (62), and might explain the lower performance of trees observed in our study. In fact, urban trees are often exposed to harsh conditions (i.e. paved soils, air pollution) which can limit transpiration and, therefore, their cooling capacity (63). However, it should be noted that the cooling effect of street trees, despite being small, is important to alleviate the UHI effect in highly urbanized areas (64).

Most of the cities that presented high UHI, were also the most densely populated (ie, Paris, Thessaloniki, Athens, Lyon, among others), with population densities ranging between 10,722 and 20,934 inhabitats per 1 km^2. Indeed, this association between population density and UHI has been well described in previous studies (10,12). Furthermore, these cities also had low TC, which indicates the potential for improving urban microclimate by increasing the urban tree layer. However, UHI formations is a complex phenomenon that have been associated with many factors. Moreover, various drivers of the UHI have differential day-time and night-time effects. While vegetation is the dominant factor for UHI intensity during day-time, the urban canyon more strongly drives UHI at night (65). On top of this, the night-time UHI intensity is on average three-fold the day-time UHI (ie, 0.6°C and 1.9°C, respectively). Therefore, UGI strategies need to be accompanied by other interventions that especially reduce night-time UHI to achieve larger health benefits, such as changing the ground surface materials (ie, asphalt to granite) and more structural interventions that involve changes in the sky view factor (ie, fraction of visible sky as the result of the street geometry and building density) (65). Indeed, our results show that, on average, 39.5% of the attributable deaths due to UHI could be avoided by increasing the TC to 30%. Evidently, and in line with other studies (66,67), this intervention should be combined with others in order to reach a greater temperature reduction and greater preventable impacts, particularly, for those cities for which increasing the TC would not reduce the temperature significantly.

Just as the characterization of the UHI is specific to each city, so is the TC cooling capacity. Our cooling estimates were not only determined by the TC cooling capacity, but by the baseline TC. In other words, if the cooling capacity is high and the baseline TC is already close to 30%, the potential for reducing temperatures through UGI would be low. In turn, if both the vegetation cooling capacity and the TC are low, the resulting potential for cooling might be higher than expected. For this reason, to improve the interpretability of our results, we built the *Cooling Efforts Index.* Notably, most cities with higher *Cooling Efforts Index* are also the ones with lower UHI attributable impacts (ie, Glasgow, Edinburg, Oslo, Göteborg, Tallin and Helsinki). On the other hand, several Mediterranean cities presented lower *Cooling Efforts Index* and tended to have, on average, greater attributable mortality impacts (ie, Athens, Valencia, Sevilla, Palermo, Málaga and Madrid). This implies that greater efforts are required for these cities, in order to achieve temperature reduction due to the combination of low baseline TC and low TC cooling capacity.

Some of the cities in semi-arid conditions also presented low or even negative UHI, however this is not due to optimal urban planning practices. In dry regions, rural land surfaces can be warmer than urban areas, particularly if the vegetation is not irrigated (68,69). Also, droughts can limit the evapotranspiration rate (62). On the other hand, urban centers with tall buildings can provide shading amplifying this negative temperature difference (70). In spite of presenting relatively low UHI intensity, in some cities (ie, Palma de Mallorca, Alicante, Porto, Roma and Napoli) the attributable mortality impacts were high. One possible explanation for this is the already high baseline temperature which poses a baseline elevated risk for the population combined with the specific association between exposure to heat and mortality (ie. ERF). For this reason, the UHI should not be the best indicator to address excess heat in these cases, as actions to mitigate general high temperatures are still needed to reduce the associated mortality impacts. Still in these settings, UGI can have an increase cooling effect if urban irrigation is used (56,71). Therefore, TC cooling capacity could be increased and would constitute a partial solution for mitigating excessive heat. However, a pitfall to consider is that urban irrigation may cause water scarcity that could be exacerbated as a result of climate change (72).

On top of this, there is the question of affordability given that trees maintenance has a greater cost under dry conditions (73). Therefore, it is important to local policy and decision-makers to consider the complete range of costs and benefits. However, in spite of the overall positive balance obtained in individual studies assessing the benefits-cost ratio of urban trees, there is no general conclusive evidence due to high variation in values, methodological differences and the limited number of studies (74). Economic valuation is important for justifying investment in urban tree planting, therefore further studies are needed in this realm (74). Furthermore, the economic valuation should also incorporate the health and social impacts which should be integrated into the decision-making framework and would probably increase the economic benefits

Urban trees provide substantial public health and public environmental benefits. However, some factors should be considered in order to maximize their potential. First, their distribution. The population-weighted-city-average TC was, on average 22% lower than the average TC without considering the population distribution, meaning that the most populated areas have less TC. In addition, previous studies have shown that urban trees are often unevenly distributed across the population, and that socioeconomically disadvantaged groups may be deprived of environmental benefits, constituting a form of environmental injustice (75). This is a reason why the intervention is proposed at a small scale enabling us to consider urban tree distribution in addition to total coverage. Nevertheless, we acknowledge that it is not always possible to meet the target in the scale used, therefore depending on the urban design, the scale of the intervention should vary. Second, planting trees in green areas (ie, parks, squares, community gardens) or grouped in central tree-lined gardens with permeable surfaces, rather than isolated street trees, may have synergic positive effects, improving not only the trees' cooling capacity but also the green spaces' quality and aesthetics, among others, hence maximizing the population health benefits (76).

The sensitivity analyses showed that the greater changes were obtained when using Martinez-Solanas et al (2021) ERFs (-17% and 21%, for the UHI scenario and 30% TC scenario respectively), which were modelled using a broader level of aggregation (ie, NUTS3), considering the entire population and with the E-obs dataset. We used an age and city-specific ERFs (16) in our main analysis, which can better reflect the population´s adaptability to ambient temperature. This is particularly important in line with evidence showing differential susceptibility associated with different age groups (ie, older adults and children have a higher risk of dying or becoming ill) (9). In addition, the ERFs also account for some socioeconomic variables, which is crucial considering that vulnerable subpopulations face greater risks of suffering from adverse health effects due to high temperatures (9). Nevertheless, we should note that we applied the same ERF across the whole city, while socioeconomic inequalities are often highly pronounced within each city population (77).

We also obtained great changes when using the city-average UHI (-18%), which were not observed, when using the summer grid-cell average UHI (+2%). This denotes that not considering the spatial variability of the UHI would lead to an underestimation of the real impacts given that often the most densely populated areas are also those with greater UHI intensity (10), which is also reflected in the mean 41% of increase obtained on the population-weighted-UHI compared to the average UHI. A similar outcome was obtained when conducting the analysis considering the city-average cooling instead of the grid-cell level cooling (-19%), emphasizing the importance of accounting for cooling spatial heterogeneity. In such a context, our analysis aims to provide spatial information of the areas that would benefit the most from targeted greening intervention in order to reduce temperatures and ameliorate living conditions of urban dwellers.

Results with alternative scenarios (-21% and +41%, for TC=25% and TC=40%, respectively) suggested a linear association between these values, which facilitates the UGI planification considering that the feasibility of the intervention should be adapted to each local setting. In fact, for cities with low availability of open public space, achieving the 30% TC target can be very challenging. Tree planting programmes will need to target private owned industrial, commercial or institutional spaces beyond publicly managed spaces (ie, streets and parks). We encourage city planners to choose a 30% TC target, however, a 25% TC could be set for compact cities facing space difficulties. In this way, a 25% TC target could also be combined with other strategies beyond tree planting, such as green roofs to reduce local temperature.

The main strengths of our study include the use of a fine spatial scale of 250 m covering 93 European cities, enabling the generation of high-resolution maps that can be used for identifying where interventions are most urgently needed, the use of city and age specific ERFs, the analysis of the attributable impacts to the UHI conducted on a daily basis and the building of a realistic city-specific counterfactual scenario that can partially mitigate the UHI impacts. Likewise, the considerable number of sensitivity analyses and the high correlation obtained between the two main analyses show the robustness of ours results.

Nevertheless, our study also has several limitations that need to be addressed. First, regarding data availability, population data was only available for 2015, which is why we could not conduct the analysis for a more recent year. Also, the mortality data was available at NUTS3 level and on weekly basis, and the age structure at a city level, which made the analysis less sensitive to within city variability and also ignore the potential weekend effects (ie, greater mortality than during weekdays) (78). Moreover, we were not able to build the uncertainty ranges for both population counts and mortality due to lack of reported errors in the published data resulting in narrower CIs. In spite of this, we were able to consider the exposure spatial variability and uncertainty in both main analyses.

We acknowledge also that this is a study for the summer 2015 meaning that the exact mortality estimations are only attributable for the reference year. However, similar mortality impacts, or even greater could be expected in the near future given that 2015 had summer temperatures similar to other years and that ongoing global warming and the intensification of UHIs might increase the impacts on health due to heat stress (40,58). Our ultimate goal is to generate a broad idea of the health benefits that could be achieved through UGI.

Moreover, we based our analysis on the resident population exposure not considering the daily commuting of people for work or study, which may lead to a misclassification of the exposure. Nevertheless, as shown in this study, night-time UHI is considerably greater than day-time UHI, therefore we consider this limitation may not represent substantial changes on the mortality impacts.

There are further limitations regarding the cooling model. First, we used an U.S dataset to build a predictive model of the relationship between surface temperature and air temperature in EU cities. Although a European dataset would have been ideal, the US one was the best option available given the insufficient coverage of the existing European weather stations network and the wide range of variables covered by the dataset. Furthermore, the model has proven to be reliable when comparing the estimated average temperature with the Urbclim temperature. A second limitation is the weak adjustment the cooling model had for some cities, which may also reflect the weak association between TC and ambient temperature. However, at the same time it enabled us to predict air temperature reduction in a simple and straightforward scalable manner through a wide spatial area. Additionally, the TC cooling capacity may depend also on other variables that were not considered in the model, such as type of trees planted (ie, leaf size and shape (79,80), height and crown width (81)). We also acknowledge that we did not account for the uncertainties each inputs of the models brought, specifically the Etree data which was obtained from another model (56,57). On top of that, a further source of uncertainties is given by the $Etree_{30}$ estimation. Although probably none of the methods used can accurately estimate evapotranspiration when TC is equal to 30%, we performed sensitivity analyses that revealed there were no significant differences between the methods used in its estimation. In spite of the cooling model limitations, the coarse-grained approach here can provide a first order guideline on expected cooling effects that is valid across the European region and that may be adjusted to specific city-settings.

We focused on the analysis of the impacts on health of high temperature, yet we need to note the potential role UHI has as low temperatures mitigator (82). Specifically, considering the current greater health impacts of cold in relation to heat in the European region (2,16,58). Nevertheless, under the global warming scenarios, the number of monthly heat records are projected to rise as well as the average temperatures. Therefore, health impacts attributable to heat are projected to exceed cold attributable health impacts in the future under high emission scenarios (58).

Finally, despite achieving a relatively low temperature reduction with the proposed UGI, the cooling obtained can prevent a considerable number of premature deaths. Here, we only estimated the preventable impacts associated with temperature reduction, whereas the full extent of urban greening health benefits should not be assessed on the basis of air cooling alone. Indeed, a previous HIA study by Pereira-Barboza et al (2021) estimated that 20 deaths per 100,000 inhabitants could be prevented annually if European cities complied with the WHO recommendation of access to green space (ie, 300m of distance to a green space from residency; using the NDVI as a proxy of greenness) (45). In spite of not using the same indicator, undoubtedly, our study and Pereira-Barboza et al. (2021) complement each other and indicate an urgent need to carry out actions to green cities for health. Urban greening also mitigates air and noise pollution (83–85), provides biodiversity, promotes population physical activity (76) and has direct impacts on physical and mental health (76,86). Further studies considering all the co-benefits of incorporating UGI in urban areas are necessary in order to demonstrate the full potential of UGI to improve environmental quality and make cities healthier, sustainable and more climate change resilient.

CONCLUSIONS

Our results showed large impacts on mortality due to the UHI in cities, and that these impacts could be partially reduced by increasing the TC in order to cool urban environments. We encourage city planners and decision-makers to incorporate the UGI adapted to each local setting whilst combining with other interventions in order to maximize the health benefits while promoting more sustainable and resilient cities.

Contributors

MN conceptualised the study idea. TI and MC worked on the study design and data collection. TI did the data analysis. TI, MC, MF, SK, EP-B, MQ-Z, and MN contributed to data interpretation. NM and MT provided input on the health impact assessment methods. MF, MH and MC contributed to the development of the Cooling model. JU and MQ-Z provided help with the R script and data management. TI wrote the manuscript. TI, SK, MC, and EP-B accessed and verified the data. All authors reviewed the manuscript and provided feedback on the study design, data analysis, and interpretation of results.

Declaration of interest

We declare no competing interests.

Data Sharing

All the data collected is routinely collected data with no information on specific people. All the data is available upon request to the corresponding author (mark.nieuwenhuijsen@isglobal.org) and with agreement of the steering group.

Acknowledgements

We acknowledge support from the Spanish Ministry of Science and Innovation and State Research Agency through the "Centro de Excelencia Severo Ochoa 2019-2023" Program (CEX2018-000806-S), and support from the Generalitat de Catalunya through the CERCA Program", GoGreenRoutes through the European Union´s Horizon 2020 Research and Innovation programme under grant agreement No. 869764. SK received funding from the Spanish Ministry of Science and Innovation through the "Ayudas para la Formación de Profesorado Universitario (FPU) 2020–24" doctoral funding (FPU19/05210). JU received funding from Spanish regional program PERIS (Ref.: SLT017/20/000119), granted by Departament de Salut de la Generalitat de Catalunya. MQZ recieved from the European Union's Horizon 2020 research and innovation programme under grant agreement No 865564 (European Research Council Consolidator Grant EARLY-ADAPT, https://early-adapt.eu/). AG received funding from the Medical Research Council-UK (Grant ID: MR/V034162/1 and MR/R013349/1) and from the European Union's Horizon 2020 Project Exhaustion (Grant ID: 820655).

References

1. Guo Y, Gasparrini A, Armstrong B, Li S, Tawatsupa B, Tobias A, et al. Global variation in the effects of ambient temperature on mortality: A systematic evaluation. Epidemiology. 2014;25(6):781–9.
2. Gasparrini A, Guo Y, Hashizume M. Mortalité attribuable au froid et à la chaleur : Analyse multi-pays. Environnement, Risques et Sante. 2015;14(6):464–5.
3. Ye X, Wolff R, Yu W, Vaneckova P, Pan X, Tong S. Ambient temperature and morbidity: a review of epidemiological evidence. Environ Health Perspect. 2012 Jan;120(1):19–28.
4. Turner LR, Barnett AG, Connell D, Tong S. Ambient temperature and cardiorespiratory morbidity: a systematic review and meta-analysis. Epidemiology. 2012 Jul;23(4):594–606.
5. Hondula DM, Barnett AG. Heat-related morbidity in brisbane, australia: spatial variation and area-level predictors. Environ Health Perspect. 2014 Aug;122(8):831–6.
6. Xu Z, Etzel RA, Su H, Huang C, Guo Y, Tong S. Impact of ambient temperature on children's health: a systematic review. Environ Res. 2012 Aug;117:120–31.
7. Lee M, Nordio F, Zanobetti A, Kinney P, Vautard R, Schwartz J. Acclimatization across space and time in the effects of temperature on mortality: A time-series analysis. Environ Heal A Glob Access Sci Source. 2014;13(1):1–9.
8. Wellenius GA, Eliot MN, Bush KF, Holt D, Lincoln RA, Smith AE, et al. Heat-related morbidity and mortality in New England: Evidence for local policy. Environ Res [Internet]. 2017;156:845–53. Available from: https://www.sciencedirect.com/science/article/pii/S0013935116312609
9. Sarofim, M.C., S. Saha, M.D. Hawkins, D.M. Mills, J. Hess, R. Horton, P. Kinney, J. Schwartz and ASJ. Temperature-Realated Death & Illness. In: The Impacts of Climate Change on Human Health in the United States: A Scientific Assessment [Internet]. 2016. p. 99–128. Available from: http://dx.doi.org/doi:10.7930/J00P0WXS
10. Oke T. The Heat Island of the Urban Boundary Layer: Characteristics, Causes and Effects. NATO ASI Ser e Appl Sci Study Inst. 1995 Jan 1;277:81–108.
11. Li F, Zheng W, Wang Y, Liang J, Xie S, Guo S, et al. Urban Green Space Fragmentation and urbanization: A spatiotemporal perspective. Forests. 2019;10(4).
12. Lee K, Kim Y, Sung HC, Jang R, Ryu J, Jeon SW. Trend analysis of urban heat island intensity according to urban area change in Asian mega cities. Sustainability. 2020;
13. Cheng W, Li D, Liu Z, Brown RD. Approaches for identifying heat-vulnerable populations and locations: A systematic review. Sci Total Environ [Internet]. 2021;799:149417. Available from: https://www.sciencedirect.com/science/article/pii/S0048969721044910
14. Heaviside C, Vardoulakis S, Cai XM. Attribution of mortality to the urban heat island during heatwaves in the West Midlands, UK. Environ Heal A Glob Access Sci Source. 2016;15(Suppl 1).
15. Dang TN, Van DQ, Kusaka H, Seposo XT, Honda Y. Green Space and Deaths Attributable to the Urban Heat Island Effect in Ho Chi Minh City. Am J Public Health [Internet]. 2018;108(S2):S137–43. Available from: https://doi.org/10.2105/AJPH.2017.304123
16. Masselot P. Excess mortality attributed to heat and cold in 801 cities in Europe. Forthcoming.
17. Murray CJL, Ezzati M, Lopez AD, Rodgers A, Vander Hoorn S. Comparative quantification of health risks: Conceptual framework and methodological issues. Popul Health Metr. 2003;1:1–20.
18. Nieuwenhuijsen M, Khreis H. Integrating human health into urban and transport planning: A framework. Integrating Human Health into Urban and Transport Planning: A Framework. 2018. 1–734 p.
19. Virk G, Jansz A, Mavrogianni A, Mylona A, Stocker J, Davies M. Microclimatic effects of green and cool roofs in London and their impacts on energy use for a typical office building. Energy Build. 2015 Feb 1;88.
20. Rosenfeld AH, Akbari H, Romm JJ, Pomerantz M. Cool communities: strategies for heat island mitigation and smog reduction. Energy Build [Internet]. 1998;28(1):51–62. Available from:

https://www.sciencedirect.com/science/article/pii/S0378778897000637

21. Tong H, Walton A, Sang J, Chan JCL. Numerical simulation of the urban boundary layer over the complex terrain of Hong Kong. Atmos Environ. 2005;39(19):3549–63.

22. Rosenzweig C, Solecki W, Parshall L, Gaffin S, Lynn B, Goldberg R, et al. Mitigating New York City's heat island with urban forestry, living roofs, and light surfaces. 86th AMS Annu Meet. 2006;(January).

23. Salamanca, Martilli A, Yagüe C. A numerical study of the Urban Heat Island over Madrid during the DESIREX (2008) campaign with WRF and an evaluation of simple mitigation strategies. Int J Climatol. 2012 Dec 1;32:2372–86.

24. Farhadi H, Faizi M, Sanaieian H. Mitigating the urban heat island in a residential area in Tehran: Investigating the role of vegetation, materials, and orientation of buildings. Sustain Cities Soc [Internet]. 2019;46:101448. Available from: https://www.sciencedirect.com/science/article/pii/S221067071831271X

25. Onishi A, Cao X, Ito T, Shi F, Imura H. Evaluating the potential for urban heat-island mitigation by greening parking lots. Urban For Urban Green [Internet]. 2010;9(4):323–32. Available from: https://www.sciencedirect.com/science/article/pii/S1618866710000403

26. Avissar R. Potential effects of vegetation on the urban thermal environment. Atmos Environ [Internet]. 1996;30(3):437–48. Available from: https://www.sciencedirect.com/science/article/pii/1352231095000135

27. Marando F, Heris MP, Zulian G, Udías A, Mentaschi L, Chrysoulakis N, et al. Urban heat island mitigation by green infrastructure in European Functional Urban Areas. Sustain Cities Soc [Internet]. 2022;77(September 2021):103564. Available from: https://doi.org/10.1016/j.scs.2021.103564

28. U. S. Environmental Protection Agency. Reducing Urban Heat Islands : Compendium of Strategies. In 2008. Available from: https://www.epa.gov/heat-islands/heat-island-compendium.

29. Ziter CD, Pedersen EJ, Kucharik CJ, Turner MG. Scale-dependent interactions between tree canopy cover and impervious surfaces reduce daytime urban heat during summer. Proc Natl Acad Sci U S A. 2019;116(15):7575–80.

30. Schwaab J, Meier R, Mussetti G, Seneviratne S, Bürgi C, Davin EL. The role of urban trees in reducing land surface temperatures in European cities. Nat Commun. 2021;12(1):1–11.

31. Konijnendijk CC. Evidence-based guidelines for greener, healthier, more resilient neighbourhoods: Introducing the 3-30-300 rule. J For Res. 2022 Aug;1–10.

32. C40 Knowledge Hub. Trees for Life: Master Plan for Barcelona's Trees 2017 - 2037 [Internet]. [cited 2022 Mar 1]. Available from: https://www.c40knowledgehub.org/s/article/Trees-for-Life-Master-Plan-for-Barcelona-s-Trees-2017-2037?language=en_US

33. Bristol Green Capital. New ambitious target launched to double city tree canopy cover by 2050 [Internet]. [cited 2022 Mar 1]. Available from: https://bristolgreencapital.org/new-ambitious-target-launched-double-city-tree-canopy-cover-2050/

34. ACT Government. Canberra'S Living Infrastructure Plan: Cooling the City Summary [Internet]. 2019. Available from: www.act.gov.au/climatechange

35. Environment Seattle Office of Sustaintability & Environment. 2016 Seattle Tree Canopy Assessment. 2016;1–18.

36. Office of Sustaintability Philadelphia. Greenworks [Internet]. Available from: https://www.phila.gov/programs/greenworks/

37. Astell-Burt T, Feng X. Association of Urban Green Space With Mental Health and General Health Among Adults in Australia. JAMA Netw open. 2019 Jul;2(7):e198209.

38. Astell-Burt T, Feng X. Urban green space, tree canopy and prevention of cardiometabolic diseases: a multilevel longitudinal study of 46 786 Australians. Int J Epidemiol. 2020 Jun;49(3):926–33.

39. United States Environmental Protection Agency (EPA). Climate Change and Heat Islands [Internet]. [cited 2022 Mar 18]. Available from: https://www.epa.gov/heatislands/climate-change-and-heat-islands

40. Huang K, Li X, Liu X, Seto KC. Projecting global urban land expansion and heat island intensification through 2050. Environ Res Lett. 2019;14(11).

41. Linstroth, T., & Bell R. Local Action: The new paradigm in Climate Change Polici. UPNE; 2007.

42. Eurostat. Database [Internet]. [cited 2021 Dec 27]. Available from: https://ec.europa.eu/eurostat/data/database

43. Copernicus. Climate variables for cities in Europe from 2008 to 2017 [Internet]. [cited 2021 Oct 20]. Available from: https://cds.climate.copernicus.eu/cdsapp#!/dataset/sis-urban-climate-cities?tab=overview

44. Khomenko S, Cirach M, Pereira-Barboza E, Mueller N, Barrera-Gómez J, Rojas-Rueda D, et al. Premature mortality due to air pollution in European cities: a health impact assessment. Lancet Planet Heal [Internet]. 2021 Feb 22; Available from: https://doi.org/10.1016/S2542-5196(20)30272-2

45. Barboza EP, Cirach M, Khomenko S, Iungman T, Mueller N, Barrera-Gómez J, et al. Green space and mortality in European cities: a health impact assessment study. Vol. 5, The Lancet Planetary Health. 2021. p. e718–30.

46. Khomenko S, Cirach M, Barrera-Gómez J, Pereira-Barboza E, Iungman T, Mueller N, et al. Impact of road traffic noise on annoyance and preventable mortality in European cities: A health impact assessment. Environ Int. 2022;162.

47. European Commission. Global Human Settlement [Internet]. 2019 [cited 2021 Sep 14]. Available from: https://ghsl.jrc.ec.europa.eu/data.php

48. Copernicus. Urban Atlas [Internet]. 2012 [cited 2021 Sep 14]. Available from: https://land.copernicus.eu/local/urban-atlas/urban-atlas-2012

49. Quijal-Zamorano M, Martínez-Solanas È, Achebak H, Petrova D, Robine JM, Herrmann FR, et al. Seasonality reversal of temperature attributable mortality projections due to previously unobserved extreme heat in Europe. Lancet Planet Heal. 2021;5(9):e573–5.

50. Eurostat. Revision of the European Standard Population. Report of Eurostat's task force. 2013.

51. Copernicus Land Monitoring Service. Tree cover density [Internet]. [cited 2022 Jan 20]. Available from: https://land.copernicus.eu/pan-european/high-resolution-layers/forests/tree-cover-density

52. Khomenko S, Nieuwenhuijsen M, Ambros A, Wegener S, Mueller N. Is a liveable city a healthy city? Health impacts of urban and transport planning in Vienna, Austria. Environ Res. 2020 Feb;183:109238.

53. Mueller N, Rojas-Rueda D, Khreis H, Cirach M, Milà C, Espinosa A, et al. Socioeconomic inequalities in urban and transport planning related exposures and mortality: A health impact assessment study for Bradford, UK. Environ Int [Internet]. 2018;121(June):931–41. Available from: https://doi.org/10.1016/j.envint.2018.10.017

54. Heris M, Bagstad KJ, Rhodes C, Troy A, Middel A, Hopkins KG, et al. Piloting urban ecosystem accounting for the United States. Ecosyst Serv [Internet]. 2021;48:101226. Available from: https://www.sciencedirect.com/science/article/pii/S2212041620301686

55. Unitaed States Geological Services (USGS). Landsat Data Access [Internet]. [cited 2021 Nov 30]. Available from: https://www.usgs.gov/landsat-missions/landsat-data-access

56. Gan R, Zhang Y, Shi H, Yang Y, Eamus D, Cheng L, et al. Use of satellite leaf area index estimating evapotranspiration and gross assimilation for Australian ecosystems. Vol. 11, Ecohydrology. 2018.

57. Zhang Y, Kong D, Gan R, Chiew FHS, McVicar TR, Zhang Q, et al. Coupled estimation of 500 m and 8-day resolution global evapotranspiration and gross primary production in 2002–2017. Remote Sens Environ [Internet]. 2019;222(May 2018):165–82. Available from: https://doi.org/10.1016/j.rse.2018.12.031

58. Martínez-Solanas È, Quijal-Zamorano M, Achebak H, Petrova D, Robine JM, Herrmann FR, et al. Projections of temperature-attributable mortality in Europe: a time series analysis of 147 contiguous regions in 16 countries. Lancet Planet Heal. 2021;5(7):e446–54.

59. Xing W, Wang W, Shao Q, Song L, Cao M. Estimation of evapotranspiration and its components across China based on a modified priestley–taylor algorithm using monthly multi-layer soil moisture data. Remote Sens. 2021;13(16).

60. Sailor DJ. Streamlined mesoscale modeling of air temperature impacts of heat island mitigation strategies. Final report Portland, OR Portl State Univ Available web cecs pdx edu/~ sailor/FinalStreamlineReportEPA2003 pdf [accessed 13 July 2006]. 2003;

61. Krayenhoff ES, Broadbent AM, Zhao L, Georgescu M, Middel A, Voogt JA, et al. Cooling hot cities: a systematic and critical review of the numerical modelling literature. Environ Res Lett. 2021;16(5).

62. Fusaro L, Salvatori E, Mereu S, Marando F, Scassellati E, Abbate G, et al. Urban and peri-urban forests in the metropolitan area of Rome: Ecophysiological response of Quercus ilex L. in two green infrastructures in an ecosystem services perspective. Urban For Urban Green [Internet]. 2015;14(4):1147–56. Available from: https://www.sciencedirect.com/science/article/pii/S1618866715001491

63. Marando F, Salvatori E, Sebastiani A, Fusaro L, Manes F. Regulating Ecosystem Services and Green Infrastructure: assessment of Urban Heat Island effect mitigation in the municipality of Rome, Italy. Ecol Modell [Internet]. 2019;392:92–102. Available from: https://www.sciencedirect.com/science/article/pii/S0304380018303995

64. Shashua-Bar L, Potchter O, Bitan A, Boltansky D, Yaakov Y. Microclimate modelling of street tree species effects within the varied urban morphology in the Mediterranean city of Tel Aviv, Israel. Int J Climatol [Internet]. 2010;30(1):44–57. Available from: https://rmets.onlinelibrary.wiley.com/doi/abs/10.1002/joc.1869

65. Chun B, Guhathakurta S. Daytime and nighttime urban heat islands statistical models for Atlanta. Environ Plan B Urban Anal City Sci [Internet]. 2015 Dec 29;44(2):308–27. Available from: https://doi.org/10.1177/0265813515624685

66. Pascal M, Goria S, Wagner V, Sabastia M, Guillet A, Cordeau E, et al. Greening is a promising but likely insufficient adaptation strategy to limit the health impacts of extreme heat. Environ Int [Internet]. 2021;151:106441. Available from: https://www.sciencedirect.com/science/article/pii/S0160412021000660

67. Kalkstein LS, Eisenman DP, de Guzman EB, Sailor DJ. Increasing trees and high-albedo surfaces decreases heat impacts and mortality in Los Angeles, CA. Int J Biometeorol [Internet]. 2022;66(5):911–25. Available from: https://doi.org/10.1007/s00484-022-02248-8

68. Gunawardena KR, Wells MJ, Kershaw T. Utilising green and bluespace to mitigate urban heat island intensity. Sci Total Environ [Internet]. 2017;584–585:1040–55. Available from: https://www.sciencedirect.com/science/article/pii/S0048969717301754

69. Cohen P, Potchter P, Matzarakis A. Daily and seasonal.climate behavior of green urban open spaces in Mediterranean climate and its impact on human comfort. Build Environ. 2013;51:294–5.

70. Memon RA, Leung DYC, Liu C-H. An investigation of urban heat island intensity (UHII) as an indicator of urban heating. Atmos Res [Internet]. 2009;94(3):491–500. Available from: https://www.sciencedirect.com/science/article/pii/S0169809509002166

71. Mariani L, Parisi SG, Cola G, Lafortezza R, Colangelo G, Sanesi G. Climatological analysis of the mitigating effect of vegetation on the urban heat island of Milan, Italy. Sci Total Environ [Internet]. 2016;569–570:762–73. Available from: http://dx.doi.org/10.1016/j.scitotenv.2016.06.111

72. He C, Liu Z, Wu J, Pan X, Fang Z, Li J, et al. Future global urban water scarcity and potential solutions. Nat Commun [Internet]. 2021;12(1):1–11. Available from: http://dx.doi.org/10.1038/s41467-021-25026-3

73. Jones BA, Fleck J. Urban Trees and Water Use in Arid Climates: Insights from an Integrated Bioeconomic-Health Model. Water Econ Policy [Internet]. 2018;04(04):1850022. Available from: https://doi.org/10.1142/S2382624X18500224

74. Song XP, Tan PY, Edwards P, Richards D. The economic benefits and costs of trees in urban forest stewardship: A systematic review. Urban For Urban Green [Internet]. 2018;29:162–70. Available from: https://www.sciencedirect.com/science/article/pii/S161886671730523X

75. Gerrish E, Watkins SL. The relationship between urban forests and income: A meta-analysis. Landsc Urban Plan. 2018 Feb;170:293–308.

76. Wolf KL, Lam ST, McKeen JK, Richardson GRA, van den Bosch M, Bardekjian AC. Urban Trees and Human Health: A Scoping Review. Int J Environ Res Public Health. 2020 Jun;17(12).

77. Lawrence RJ. Urban health challenges in Europe. J Urban Health. 2013 Oct;90 Suppl 1(Suppl 1):23–36.

78. Freemantle N, Richardson M, Wood J, Ray D, Khosla S, Shahian D, et al. Weekend hospitalization and additional risk of death: an analysis of inpatient data. J R Soc Med. 2012 Feb;105(2):74–84.

79. Tamaskani Esfehankalateh A, Ngarambe J, Yun GY. Influence of tree canopy coverage and leaf area density

on urban heat island mitigation. Sustain. 2021;13(13).

80. Gillner S, Vogt J, Tharang A, Dettmann S, Roloff A. Role of street trees in mitigating effects of heat and drought at highly sealed urban sites. Landsc Urban Plan [Internet]. 2015;143:33–42. Available from: https://www.sciencedirect.com/science/article/pii/S0169204615001309

81. Fu J, Dupre K, Tavares S, King D, Banhalmi-Zakar Z. Optimized greenery configuration to mitigate urban heat: A decade systematic review. Front Archit Res [Internet]. 2022;11(3):466–91. Available from: https://www.sciencedirect.com/science/article/pii/S209526352100100X

82. Macintyre HL, Heaviside C, Cai X, Phalkey R. The winter urban heat island: Impacts on cold-related mortality in a highly urbanized European region for present and future climate. Environ Int [Internet]. 2021;154:106530. Available from: https://www.sciencedirect.com/science/article/pii/S0160412021001550

83. Selmi W, Weber C, Rivière E, Blond N, Mehdi L, Nowak D. Air pollution removal by trees in public green spaces in Strasbourg city, France. Urban For Urban Green [Internet]. 2016;17:192–201. Available from: https://www.sciencedirect.com/science/article/pii/S1618866716301571

84. Jim CY, Chen WY. Assessing the ecosystem service of air pollutant removal by urban trees in Guangzhou (China). J Environ Manage. 2008;88(4):665–76.

85. Urban Green Blue. Trees as Sound Barriers. Green Blue Urban. 2015;5–8.

86. Browning MHEM, Lee K, Wolf KL. Tree cover shows an inverse relationship with depressive symptoms in elderly residents living in U.S. nursing homes. Urban For Urban Green [Internet]. 2019;41:23–32. Available from: https://www.sciencedirect.com/science/article/pii/S1618866718306678

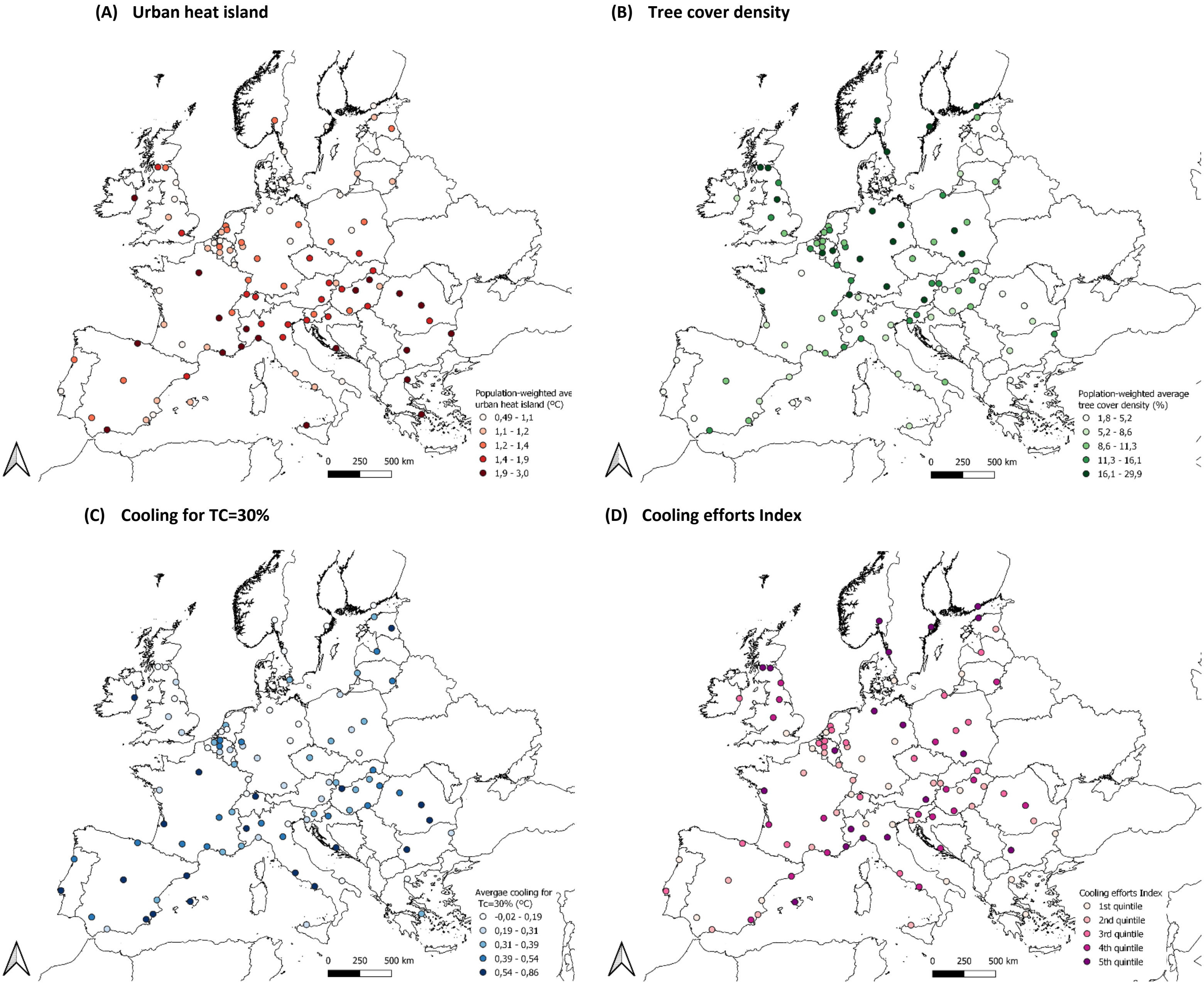

Figure 1. *Distribution of population-weighted-average urban heat island, population-weighted-average tree cover density, cooling capacity for TC=30% and Cooling efforts index among European cities.*

(A) UHI attributable mortality rates

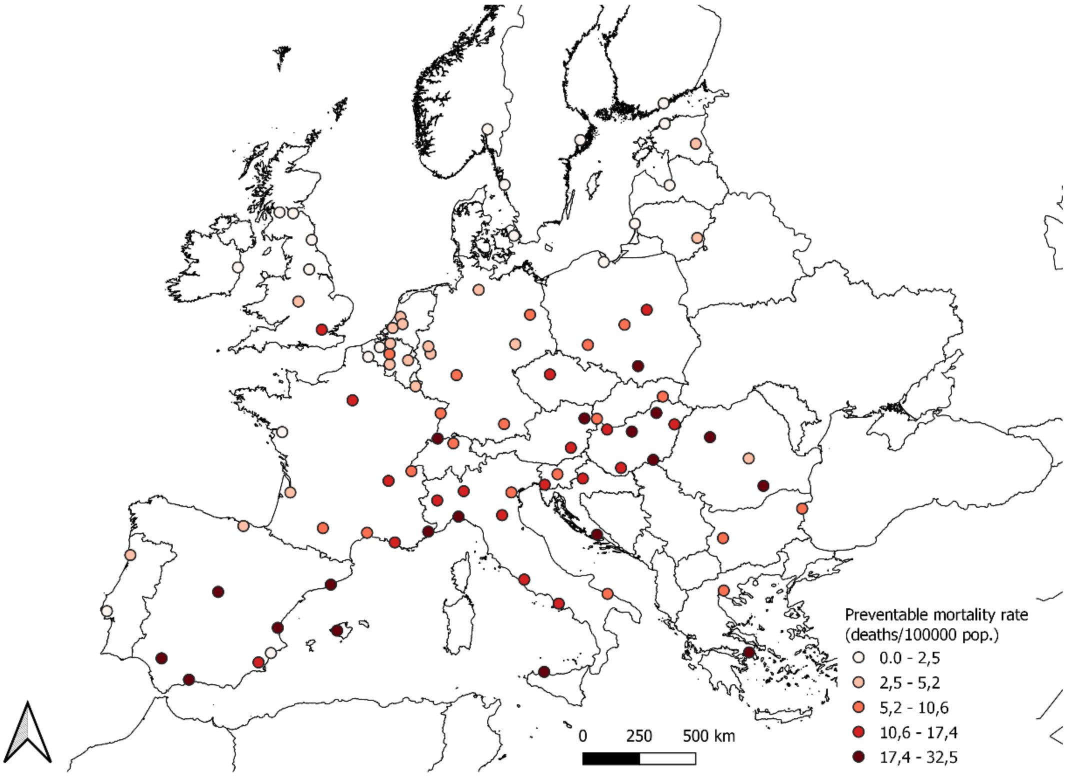

(B) Preventable mortality rates (for TC=30%)

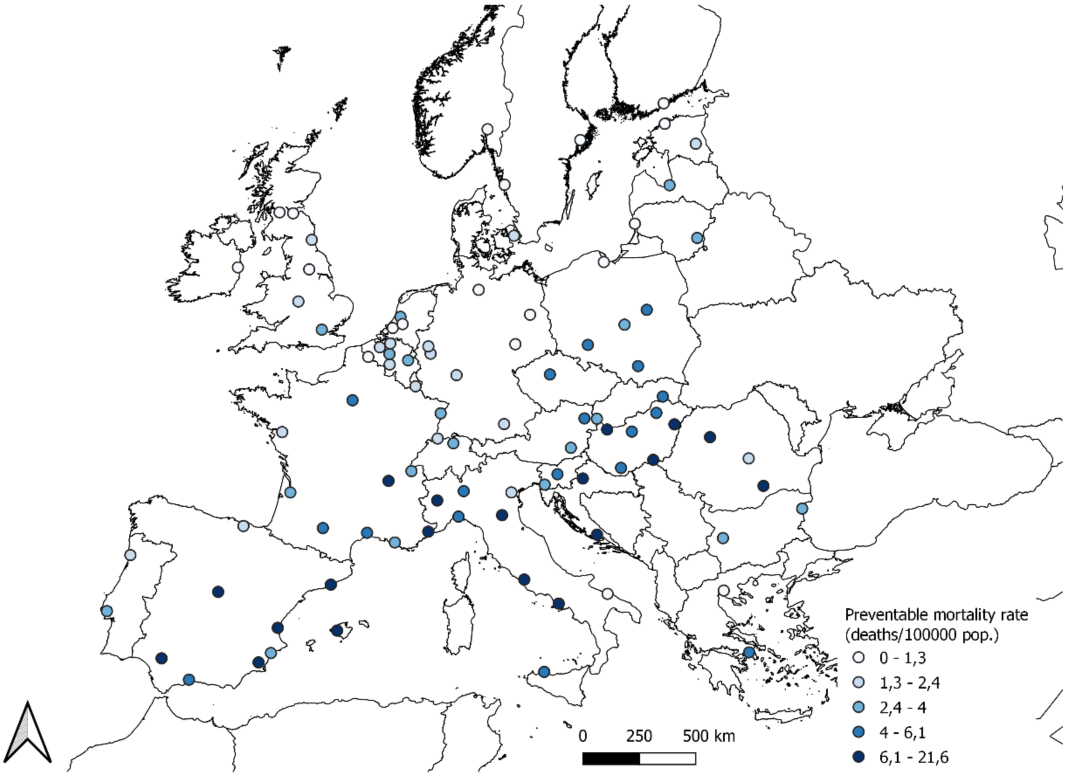

Figure 2. *Distribution of average standardized mortality rates attributable to UHI and preventable under the urban green interventions.*

Table 1. *Results of the health impact assessment for the main analyses and sensitivity analyses*

	Exposure-response function (ERF)	Summer preventable deaths (n; 95% CI)	Summer preventable age-standardized mortality rate (deaths/100,000 inhabitants, 95% CI)	Summer preventable impact on deaths (%; 95% CI)	Annual preventable impact on deaths (%; 95% CI)	Year of life lost (per 100,000 inhaitants. 95% CI)	Change (%)
Urban Heat Island							
Main	**Masselot et al (Forthcoming)**	**6,700 (5,254 - 8,162)**	**9.91 (7.71 - 12.07)**	**4.33 (3.37 - 5.28)**	**0.90 (0.67 - 1.11)**	**166.42 (128.47 - 201.98)**	-
Sensitivity							
Using mean summer UHI per grid cell	**Masselot et al (Forthcoming)**	6,854 (6,196 - 7,494)	10.10 (9.08 - 11.00)	4.42 (3.98 - 4.82)	0.90 (0.76 - 0.99)	169.78 (148.98 - 185.44)	**+2%**
Using mean UHI per city	**Masselot et al (Forthcoming)**	5,478 (0 - 11,742.28)	8.08 (0.00 - 17.45)	3.51 (0.00 - 7.68)	0.72 (0.00 - 1.66)	135.90 (0.00 - 288.61)	**-18%**
Using the adjusted annual city mortality dataset	**Masselot et al (Forthcoming)**	6,933 (5,434 - 8,483)	10.09 (7.80 - 12.33)	4.46 (3.43 - 5.48)	0.93 (0.68 - 1.15)	142.68 (111.95 - 171.82)	**+3%**
Using the non-adjusted annual city mortality dataset	**Masselot et al (Forthcoming)**	8,061 (6,319 - 9,864)	11.73 (9.08 - 14.33)	5.19 (3.99 - 6.37)	0.86 (0.65 - 1.04)	165.91 (130.18 - 199.79)	**+20%**
Using another ERF [1]	**Martinez-Solanas et al (2021)**	4,401 (3,779 - 5,056)	10.18 (8.75 - 11.65)	4.86 (4.18 - 5.56)	1.17 (0.99 - 1.37)	185.76 (159.65 - 211.70)	**-17%**
Cooling							
Main	**Masselot et al (Forthcoming)**	**2,644 (2,444 - 2,824)**	**4.17 (3.83 - 4.49)**	**1.84 (1.69 - 1.97)**	**0.37 (0.32 - 0.41)**	**69.85 (62.36 - 75.67)**	-
Sensitivity							
Using mean cooling per city	**Masselot et al (Forthcoming)**	2,148 (792 - 3,472)	3.21 (0.77 - 5.54)	1.42 (0.38 - 2.43)	0.29 (0.06 - 0.50)	54.06 (15.05 - 91.53)	**-19%**
Using another ERF [1]	**Martinez-Solanas et al (2021)**	1,694 (1,580 - 1,811)	3.96 (3.68 - 4.23)	1.87 (1.74 - 2.00)	0.46 (0.42 - 0.50)	72.49 (67.56 - 77.59)	**-21%**
Using a linerar regression by city for the Etree$_{30}$ estimation	**Masselot et al (Forthcoming)**	2,667 (2,466 - 2,861)	4.19 (3.86 - 4.51)	1.84 (1.70 - 1.98)	0.37 (0.32 - 0.40)	70.24 (62.91 - 76.05)	**+1%**
Using a linerar regression by biome for the Etree$_{30}$ estimation	**Masselot et al (Forthcoming)**	2,687 (2,477 - 2,888)	4.21 (3.85 - 4.54)	1.87 (1.72 - 2.02)	0.38 (0.32 - 0.41)	71.17 (63.30 - 76.90)	**+3%**
Additional analysis							
Using as counterfactual Tc=25%	**Masselot et al (Forthcoming)**	2,092 (1,933 - 2,241)	3.32 (3.05 - 3.58)	1.46 (1.34 - 1.57)	0.29 (0.25 - 0.32)	55.62 (49.46 - 60.18)	**-21%**
Using as counterfactual Tc=40%	**Masselot et al (Forthcoming)**	3,727 (3,462 - 3,992)	5.83 (5.38 - 6.26)	2.58 (2.38 - 2.76)	0.51 (0.44 - 0.56)	97.85 (87.77 - 105.99)	**+41%**

[1] For the 66 cities covered

Table 2. *Main health impact assessment results of the urban heat island in ten European cities with the lowest (top) and the highest (bottom) attributable mortality impacts.*

City Name	Mean summer temperature (ºC)	Average Urban Heat Island (ºC)	Population-weighted average Urban Heat Island (ºC)	Percentage of population exposed to more than 1º of UHI	Summer attributable deaths (n; 95% CI)	Attributable age-standardized mortality rate (deaths/100,000 inhabitants, 95% CI)	Summer preventable impact on deaths (%; 95% CI)
Stockholm	16.68	0.34	0.49	0.11	0.00 (-10.00 - 8.72)	0.00 (-1.73 - 1.48)	0.00 (-0.84 - 0.73)
Göteborg	15.93	0.44	0.63	6.84	0.00 (-4.03 - 2.69)	0.00 (-0.88 - 0.59)	0.00 (-0.47 - 0.32)
Newcastle	15.13	0.72	0.78	23.54	0.89 (-2.51 - 4.72)	0.38 (-1.11 - 2.05)	0.16 (-0.46 - 0.86)
Leeds	15.08	0.42	0.63	14.29	3.32 (-6.23 - 13.92)	0.63 (-1.31 - 2.76)	0.28 (-0.53 - 1.19)
Tallinn	16.38	0.95	1.11	75.19	2.13 (-0.56 - 4.30)	0.73 (-0.17 - 1.44)	0.29 (-0.08 - 0.60)
Cluj-Napoca	23.09	2.43	3.00	95.67	71.12 (65.49 - 77.05)	32.49 (29.89 - 35.14)	10.36 (9.54 - 11.23)
Málaga	27.75	1.91	2.42	98.76	112.69 (100.53 - 124.59)	27.29 (24.32 - 30.20)	12.39 (11.05 - 13.70)
Barcelona	25.82	1.09	1.47	76.70	362.96 (312.73 - 405.94)	26.69 (22.91 - 30.02)	14.82 (12.77 - 16.58)
Budapest	24.82	1.60	1.90	93.95	378.10 (316.06 - 425.43)	25.71 (21.34 - 28.92)	8.77 (7.33 - 9.86)
Palma de Mallorca	27.06	0.88	1.17	73.21	69.50 (57.37 - 81.00)	23.87 (19.57 - 27.94)	11.99 (9.90 - 13.97)

Table 3. *Main health impact assessment results of the TC=30% scenario in ten European cities with the lowest (top) and the highest (bottom) preventable mortality impacts.*

City Name	Average tree cover density (%)	Population-weighted average tree cover density (%)	Average tree cover density increment (%)	Average cooling (ºC)	Maximum cooling (ºC)	Summer preventable deaths (n; 95% CI)	Annual preventable age-standardized mortality rate (deaths/100,000 inhabitants, 95% CI)	Summer preventable impact on deaths (%; 95% CI)
Oslo	34.62	29.42	3.76	0.10	0.81	0.01 (-0.56 - 0.67)	0.00 (-0.15 - 0.17)	0.00 (-0.07 - 0.09)
Bari	15.83	8.99	14.08	-0.02	0.47	0.26 (0.01 - 0.45)	0.09 (0.01 - 0.16)	0.05 (0.00 - 0.09)
Glasgow	19.02	17.29	11.97	0.04	0.24	0.61 (0.42 - 0.77)	0.15 (0.11 - 0.19)	0.05 (0.03 - 0.06)
Lille	12.97	15.26	16.11	0.01	0.22	0.90 (0.72 - 1.08)	0.17 (0.14 - 0.20)	0.07 (0.06 - 0.09)
Edinburgh	25.36	25.48	5.40	0.02	0.33	0.62 (0.43 - 0.80)	0.18 (0.12 - 0.23)	0.08 (0.05 - 0.10)
Palma de Mallorca	8.03	5.15	23.03	0.68	1.04	62.56 (61.31 - 63.72)	21.60 (21.19 - 22.00)	1.95 (1.91 - 1.99)
Barcelona	8.41	5.39	23.31	0.70	0.89	214.52 (205.60 - 220.98)	15.84 (15.16 - 16.33)	1.69 (1.62 - 1.74)
Split	5.40	1.79	25.93	0.79	1.04	14.72 (13.95 - 15.38)	12.44 (11.80 - 12.99)	0.71 (0.67 - 0.74)
Naples	13.05	6.37	19.67	0.64	1.00	75.77 (72.14 - 79.34)	11.28 (10.72 - 11.81)	0.98 (0.93 - 1.02)
Murcia	10.31	8.85	20.83	0.66	1.25	29.85 (29.04 - 30.60)	10.60 (10.31 - 10.86)	0.96 (0.93 - 0.98)

THE LANCET

Supplementary appendix 1

This appendix formed part of the original submission and has been peer reviewed. We post it as supplied by the authors.

Supplement to: Iungman T, Cirach M, Marando F, et al. Cooling cities through urban green infrastructure: a health impact assessment of European cities. *Lancet* 2023; published online Jan 31. https://doi.org/10.1016/S0140-6736(22)02585-5.

COOLING CITIES FOR HEALTH THROUGH GREEN INFRASTRUCTURE:

A HEALTH IMPACT ASSESSMENT FOR EUROPEAN CITIES

Tamara Iungman[1,2,3], Marta Cirach[1,2,3], Federica Marando[4], Evelise Pereira Barboza[1,2,3], Sasha Khomenko[1,2,3], Pierre Masselot[5], Marcos Quijal-Zamorano[1,2], Natalie Mueller[1,2,3], Antonio Gasparrini[5,6,7], José Urquiza[1,2,3], Mehdi Heris[8], Meelan Thondoo[1,9], Mark Nieuwenhuijsen[1,2,3]

1 Institute for Global Health (ISGlobal), Barcelona, Spain

2 Department of Experimental and Health Sciences, Universitat Pompeu Fabra, Barcelona, Spain

3 CIBER Epidemiología y Salud Pública (CIBERESP), Madrid, Spain

4 European Commission – Joint Research Centre, Ispra, Italy

5 Department of Public Health, Environments and Society, London School of Hygiene and Tropical Medicine (LSHTM), London, UK

6 Centre on Climate Change and Planetary Health, London School of Hygiene & Tropical Medicine (LSHTM), London, UK

7 Centre for Statistical Methodology, London School of Hygiene & Tropical Medicine (LSHTM), London, UK

8 Hunter College City University of New York

9 MRC Epidemiology Unit, University of Cambridge School of Clinical Medicine, Cambridge, UK

Correspondence to:

Prof. Mark Nieuwenhuijsen,

ISGlobal, 08003, Barcelona, Spain

mark.nieuwenhuijsen@isglobal.org

Content

List of acronyms

CI	Confidence interval
CRA	Comparative risk assessment
CVD	Cardiovascular disease
ERF	Exposure-response function
ESP	European standard population
Etree	Water evaporated from trees
FUA	European Functional Urban Area
GHSL	Global Human Settlement Layer
HIA	Health impact assessment
LST	Land Surface Temperature
NCD	Non-communicable diseases
NDVI	Normalized difference vegetation index
NUTS	Nomenclature of Territorial Units for Statistics
PAF	Population Attributable Fraction
PML	Penman-Monteith-Leuning
RMSE	Root mean squared error
Tair	Maximum air temperature
TC	Tree cover
UGI	Urban green infrastructure
UHI	Urban heat island
UrbClim	Urban Climate model
WHO	World Health Organization
YLL	Years of Life Lost

Evidence before the study

We did two different literature searches in PubMed, Scopus, and Google Scholar. For the first one, our search terms were: "urban heat island" AND "mortality" OR "premature mortality" AND "impact assessment" OR "health impact". For the second one our search terms were: "green spaces" OR "green areas" OR "urban green infrastructure" OR "tree cover" OR "tree coverage" OR "tree canopy" OR "urban trees" AND "cooling" OR "temperature reduction" OR "heat mitigation" AND "mortality" OR "premature mortality" AND "impact assessment" OR "health impact"

Supplement A. City definition

City definition

We retrieved the European cities from the Urban Audit (UA) 2018 dataset (1). The city definition was based on the presence of an “urban centre”, which is defined as followed: (1) Selection of grid cells with population density over 1,500 inhabitants/km^2; (2) Clustering of contiguous high-density cells and selection of clusters with a population above 50,000 inhabitants as the “urban centre”; (3) Defining cities as the local administrative units with at least half their population in an “urban centre”. For urban centres that extends far beyond the city, a ‘greater city’ level was created (2).

Supplement B. Demographic data

a) Population data

The Global Human Settlement Layer (GHSL) method combines information from population censuses and downscales the population into grid cells of 250m by 250m resolution, based on the presence or absence of built-up area in the grid cell (3). We reduced the GHSL reference dataset to only those grid cells that covered residential areas to better represent population distribution, to avoid locating inhabitants in non-residential areas (eg. industrial zones, port areas, airports). We retrieve land use data from the European Urban Atlas 2012 and retain grid cells that intersect with any of the residential categories defined in the Urban Atlas (i.e. Continuous Urban Fabric, Discontinuous Dense Urban Fabric, Discontinuous Medium-Density Urban Fabric, Discontinuous Low-Density Urban Fabric and Discontinuous Very Low-Density Urban Fabric) (4).

Given that the UrbClim data was available at a gridded raster, for some cities the overlap with the Urban Audit layer was not exact and as a result there were city grid-cells with no temperature data which were excluded from the analysis (ie, a city-average equal to 97.7% of population covered) (a full list with the percentage of grids and population covered is available in the Supplementary Table 1).

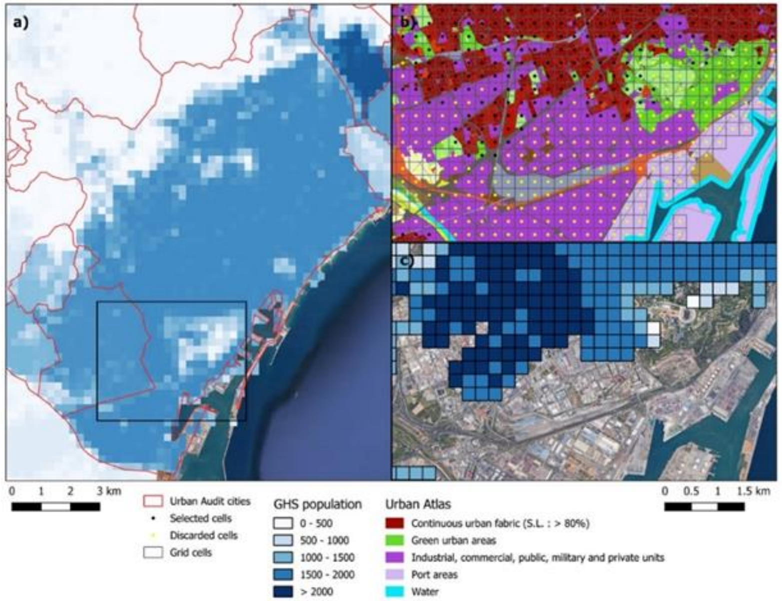

Figure S1: *Example of procedure applied for the population redistribution (example: Barcelona area): a) original population raster from GHSL, b) selection of cells based on residential land uses, and c) final dataset with weighted population redistribution assigned for each cell*

b) *Age distribution*

The population age distribution for 2015 was obtained from Eurostat at the Nomenclature of Territorial Units for Statistics (NUTS) 3 level (5,6). We retrieved the population data by age group (i.e. 20-24, 25-29, 30-34, 35-39, 40-44, 45-49, 50-54, 55-59, 60-64, 65-69, 70-74, 75-79, 80-84 and 85 years and older) and calculated the proportion of the population per age group. We assumed the same age distribution between the NUTS3-level and the corresponding city level. The population age proportions of each city were applied to the total population counts in the corresponding grid cells to estimate the population by age group for each grid cell and the city-level adult population count. After that, we aggregated the groups as 20-44, 45-64, 65-74, 75-84 and 85 years and older to fit them with ERFs.

c) *Mortality data*

We retrieved weekly all-cause mortality counts by age group for 2015 from Eurostat (7) for 81 cities at NUTS3 level. We estimated the daily mortality rates per age group per city assuming an homogeneous distribution of deaths over the same week and applied the rates to each grid cell.

For cities without weekly deaths counts available (ie, Berlin, Dusseldorf, Frankfurt, Hamburg, Koln, Leipzig, Ljubljana, Munich, Prague, Split, Zagreb) we retrieved annual city-specific all-cause mortality counts for 2015 from Eurostat (7). For only one city (ie, Dublin) we estimated the total all-cause mortality count using the country-level age-specific all-cause mortality rates, which was also available through the Eurostat database. We estimated the mortality rates per age group and applied the rates to each grid cell. We retrieved monthly country mortality counts (7) and estimated the proportion of deaths per month. We assumed an homogeneous distribution of deaths over the same month and estimated the daily deaths per grid cell.

For the 81 cities with weekly mortality data, we also retrieved annual city-specific all-cause mortality and followed the same procedure as described before for comparison. On average, the death counts estimated with the annual city-specific dataset were 17% higher with a Pearson correlation equal to 0.98. We ran a linear regression between both data sets (Table S1) and adjusted the annual mortality dataset by applying a calibration of 86%.

		p-value
Intercept	-10.34	0.766
Coefficient	0.86	< 2.2e-16

Table S1. *Linear regression coefficients and p-values for the association between the annual city-specific dataset and the weekly NUTS3 dataset.*

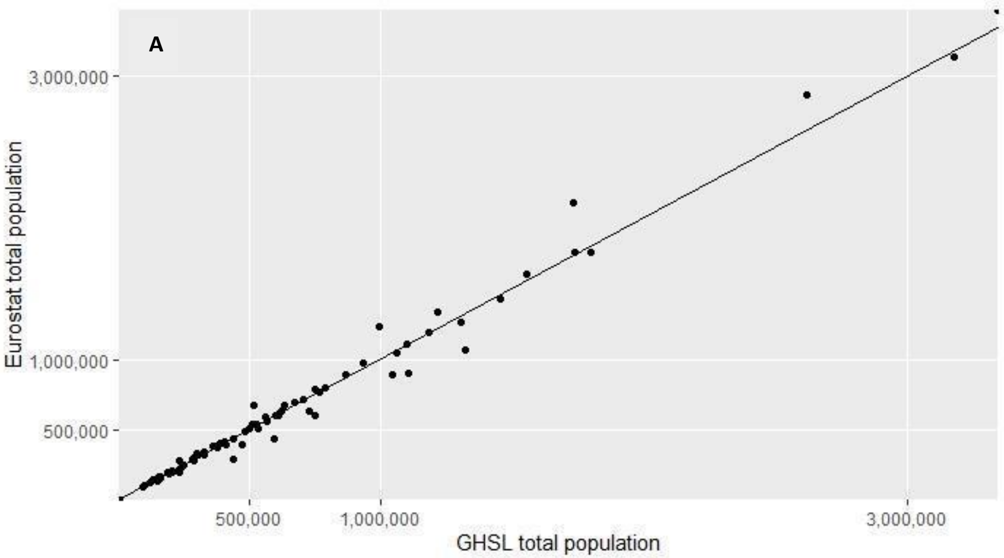

Figure S2: (A) *Association between GHSL total population and Eurostat total population. (Pearson correlation=0.99).* ***(B)*** *Association between summer all-cause deaths counts estimations from city level annual deaths counts and from NUTS3 level weekly deaths counts. (Pearson correlation=0.98).* ***(C)*** *Association between adjusted summer all-cause deaths counts estimations from city level annual deaths counts and from NUTS3 level weekly deaths counts. (Pearson correlation=0.98).*

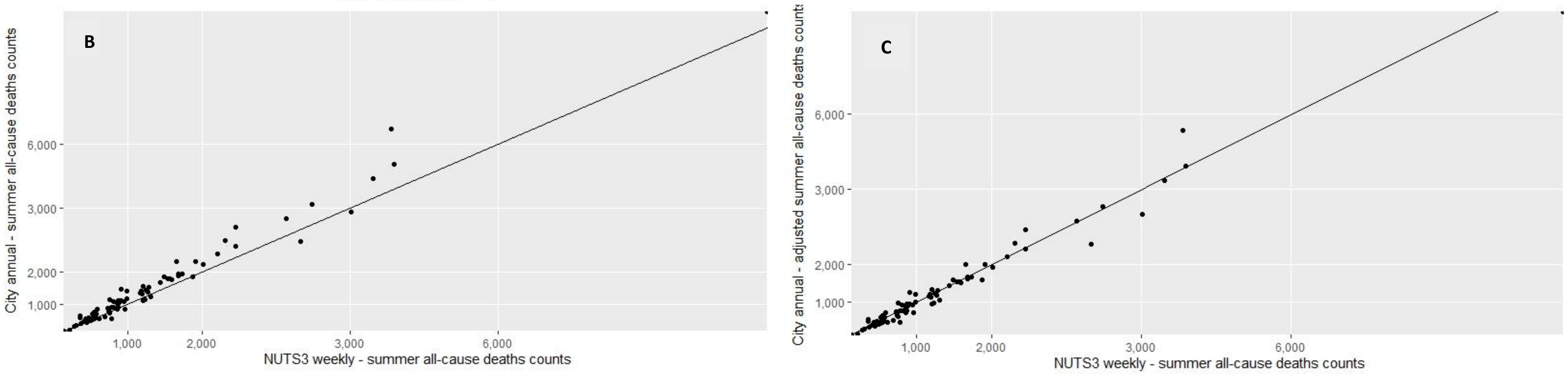

Supplement C. Health Impact Assessment (HIA)

We have analysed the historical average summer temperature according to the Köppen–Geiger climate zones to check whether 2015 was a normal year. We did not identify 2015 as an abnormal temperature year, however we observed an overall light increase trend (Figure S3).

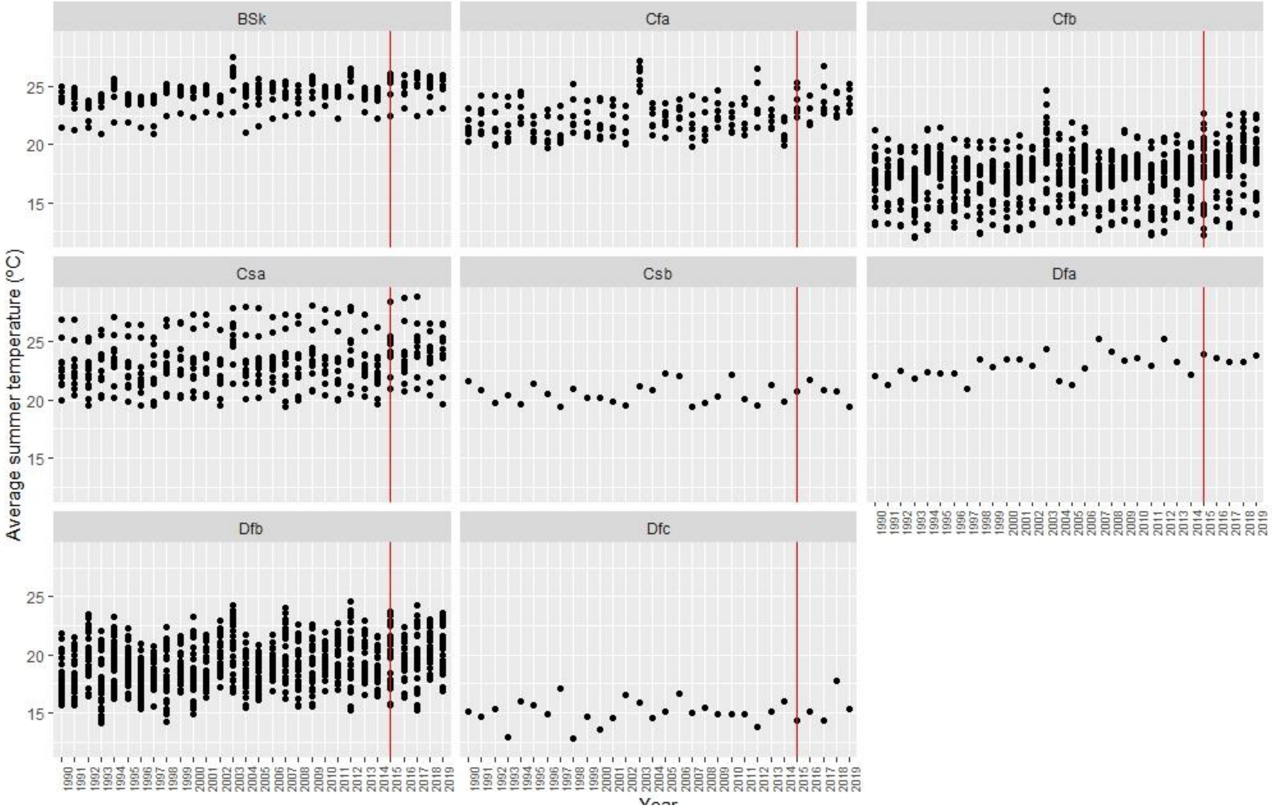

Figure S3. Average summer temperature by climate zone from 1991 to 2019. The red line indicates 2015, the baseline year for the analysis BSk = Arid, steppe, cold; Cfa= Temperate, no dry season, hot summer; Cfb= Temperate, no dry season, warm summer; Csa= Temperate, dry summer, hot summer; Csb= Temperate, dry summer, warm summer; Dfa= Cold, no dry season, hot summer; Dfb= Cold, no dry season, warm summer; Dfc= Cold, no dry season, cold summer

We retrieved city and age group-specific exposure-response functions (ERFs) from Masselot et al 2021 (8). We estimated the daily baseline temperature exposure levels and we assigned to each age group a RR accordingly. We calculated the Population Attributable Fraction (PAF) for each daily mean temperature (i) and age group (j) at a grid-cell level (k) as:

$$\textbf{Eq. (S2)} \qquad \mathbf{PAF_{ijk}=RR_{ijk}-1/RR_{ijk}}$$

The PAF is the proportional reduction in population mortality that would occur if temperature were reduced to the corresponding 'Minimum mortality temperature (MMT)' (ie, the mean daily temperature at which the lowest mortality occurs) (9).

We estimated the attributable premature mortality burden combining the PAF and the daily natural-cause mortality. We repeated the same procedure for each of the counterfactual scenarios and we calculated the difference with the baseline scenario. The obtained result is the premature mortality burden attributed to shifting baseline exposure levels to the specific counterfactual exposure level scenario (Figure S4).

We added up the results by city and age groups and estimated the preventable age-standardized mortality per 100,000 population, based on European Standard Population (ESP) (10) and the percentage of preventable annual and summer all-cause deaths. Additionally, we calculated the Years of Life Lost (YLL) due to the premature deaths as:

$$\textbf{Eq. (S3)} \qquad \mathbf{YLL = Attributable\ deaths_{\ age\ group} * Life\ expectancy_{\ age\ of\ death}}$$

YLL is a measure of premature mortality that considers both the frequency of deaths and the age at which it occurs. The YLLs for a cause are essentially calculated as the number of deaths from the specific cause multiplied by a loss function specifying the years lost for deaths as a function of the age at which death occurs. The average age at death was estimated as the mean age of each age group by city and the standard life expectancy at the age of death was obtained from country-level life tables available through Eurostat (11). YLL depends on an age weighting that encodes how the value of life is distributed with age, and on a time discount rate that represents a possible decreasing value of future lives. In this study, we applied a uniform age weighting and a 0%-time discount rate following the GBD and WHO approach to count years lived equally at all ages now and in the future (ie, giving an equal weight to years of healthy life lost at young ages and older ages) (12).We performed the analysis considering the sources of uncertainty. We built the range of uncertainty for each of the parameters involved in the mortality impacts estimations based on their SE and assuming a normal distribution. We then conducted 500 Monte Carlo iterations by sampling from the built ranges at a grid-cell level. From each sampling we aggregated the results to a city level, therefore we ended up with 500 results for each city, from which we estimated the mean (point estimate) and 2.5 and 97.5 percentiles (95% CI) for each city.

For building the temperature and the UHI uncertainty ranges (both datasets with daily and gridded variability) we considered a sample by day (ie, same error for all of the grids for each day) for avoiding errors from cancelling each other out.

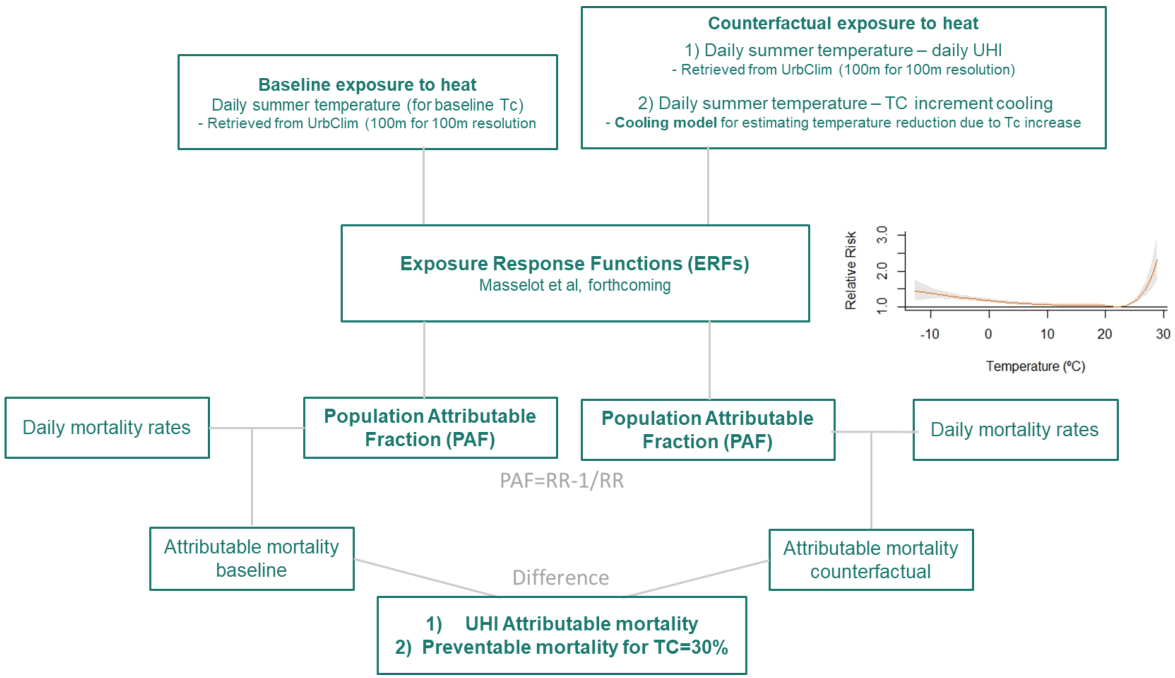

***Figure S4**. Summarised methodological steps of the Health Impact Assessment analysis.*

Association between UHI HIA and TC=30% HIA

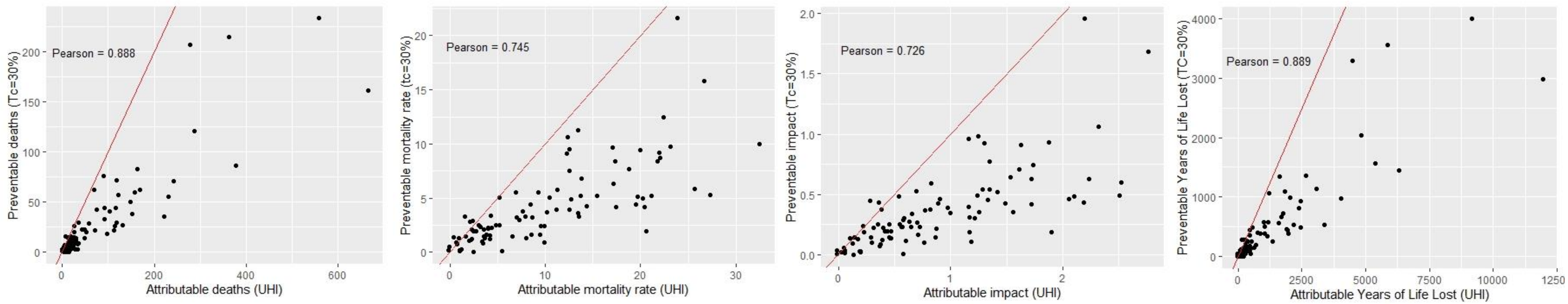

Supplement D. Exposure Response Function (ERF)

We generated city and age-specific ERFs from the framework of Masselot et al (forthcoming). The authors developed a three-stage analysis design to map ERFs across Europe. Very briefly, first, they estimated the city-specific overall cumulative exposure-response function in cities with observed daily mortality data through a quasi-Poisson regression model accounting for non-linearity and lagged effects. Secondly, they created a predictive model by conducting a meta-regression of the first-stage ERF coefficients using age, regional indicator and city-specific characteristics. This meta-regression model can then be used to predict ERF for any age group and any city in Europe (1).

Given that the risk estimates were built under the ERA5-LAND temperature dataset with a resolution of approximately 9 km, therefore covering rural areas, it was expected that the ERF temperature range was lower than the UrbClim temperature range. For that reason, we applied a city-specific correction to the UrbClim dataset as:

Eq. (S1) $\mathbf{T_{urbclim} = \alpha + \beta * T_{era5}}$

Where $T_{urbclim}$ is the mean UrbClim daily city-level temperature and T_{era5} is the mean ERA5-LAND daily city-level temperature for 2015.

We then ran Eq1´ at a grid cell-level with their corresponding city-specific coefficients.

Eq. (S1´) $\mathbf{T_{urbclim\ adjusted} = (T_{urbclim} - \alpha) / \beta}$

Table S2. Statistical distribution of Equation 1 coefficients and determinant coefficient (R^2)

α	**β**	**R^2**
-1.22 ± 0.95	-0.98 ± 0.03	0.98 ± 0.01

After adjusting the temperature dataset, there were still some days with temperature values falling out of the ERFs (ie, temperature values above the maximum temperature with an estimated risk). We chose a conservative approach and instead of extrapolating the ERFs above the maximum, we assigned to highest temperatures, the corresponding maximum temperature´ risk available (Table S3).

Table S3. *Maximum exposure-response function predictive values and maximum UrbClim values at a grid-cell level (250m). Adjustment equation applied to each city.*

City name	City code	Maximum ERF predictive values (ºC)	Maximum summer temperature UrbClim (250m)	Difference (ºC)	Alfa	Beta	error	R squared
Wien	AT001C1	28.885	32.28	3.395	-1.24	1.00	0.90	0.99
Graz	AT002C1	25.559	30.738	5.179	-2.35	1.00	0.76	0.99
Bruxelles / Brussel	BE001C1	26.563	29.928	3.365	-1.22	0.98	0.77	0.98
Antwerpen	BE002C1	26.319	29.095	2.777	-0.84	0.98	0.73	0.98
Gent	BE003C1	26.815	28.863	2.047	-0.30	1.00	0.59	0.99
Charleroi	BE004C1	26.373	29.062	2.689	-0.67	0.97	0.74	0.98
Liège	BE005C1	26.904	31.338	4.433	-0.88	0.98	0.73	0.99
Sofia	BG001C1	31.871	30.58	-1.291	-2.57	1.03	1.03	0.99
Varna	BG003C1	30.402	31.39	0.987	-0.97	0.96	0.75	0.99
Zürich	CH001C1	27.747	32.652	4.906	-1.96	0.96	0.97	0.98
Genève	CH002C1	27.559	31.756	4.196	-3.40	1.04	1.03	0.98
Basel	CH003C1	24.628	32.582	7.954	-3.03	0.99	1.00	0.98
Praha	CZ001C1	28.369	32.19	3.821	-0.62	0.99	0.53	1.00
Berlin	DE001C1	27.598	33.055	5.457	-1.05	0.99	0.74	0.99

Hamburg	DE002C1	26.425	29.404	2.979	-0.52	0.97	0.67	0.99
München	DE003C1	27.548	31.115	3.567	-1.85	0.98	1.28	0.97
Köln	DE004C1	28.414	31.656	3.242	-0.90	0.98	0.52	0.99
Frankfurt am Main	DE005C1	28.861	33.643	4.781	-1.65	0.99	0.90	0.98
Leipzig	DE008C1	29.899	31.544	1.646	-0.50	0.96	0.77	0.99
Düsseldorf	DE011C1	28.448	31.057	2.609	-0.69	0.99	0.54	0.99
København	DK001C1	24.295	28.48	4.185	-0.67	0.96	0.61	0.99
Tallinn	EE001C1	25.308	22.725	-2.583	-0.41	0.99	0.40	1.00
Tartu	EE002C1	25.775	23.979	-1.797	-0.41	0.99	0.40	1.00
Athina	EL001C2	32.653	36.119	3.465	-2.31	0.95	1.32	0.97
Thessaloniki	EL002C2	32.336	33.997	1.661	-2.90	0.98	0.71	0.99
Madrid	ES001C1	26.26	35.15	8.89	-2.74	1.02	1.12	0.98
Barcelona	ES002C1	24.523	31.625	7.102	-2.04	1.00	0.50	0.99
Valencia	ES003C1	24.577	33.633	9.056	-1.97	1.01	0.70	0.99
Sevilla	ES004C1	25.198	35.719	10.521	-1.52	1.01	0.58	0.99
Málaga	ES006C1	26.504	36.295	9.791	-1.50	0.94	0.54	0.99
Murcia	ES007C1	27.01	34.025	7.015	-0.40	0.95	0.45	1.00
Palma de Mallorca	ES010C1	23.231	31.785	8.554	-0.11	0.96	0.56	0.99
Bilbao	ES019C1	28.18	28.813	0.633	-0.10	0.91	0.61	0.98
Alicante/Alacant	ES021C1	31.628	32.547	0.919	0.38	0.94	0.57	0.99
Helsinki / Helsingfors	FI001C2	24.962	23.247	-1.715	-1.59	1.01	0.74	0.99
Paris	FR001C1	28.49	33.547	5.057	-2.75	0.99	1.13	0.97
Lyon	FR003C2	28.486	33.971	5.485	-2.12	1.02	0.96	0.98
Toulouse	FR004C2	29.287	30.758	1.472	-0.81	1.00	0.66	0.99
Strasbourg	FR006C2	27.683	35.122	7.44	-2.27	1.00	0.68	0.99
Bordeaux	FR007C1	30.57	32.196	1.626	-1.06	1.00	0.57	0.99
Nantes	FR008C1	28.628	29.779	1.15	0.02	0.96	0.53	0.99
Lille	FR009C1	29.83	29.613	-0.218	-0.76	0.99	0.67	0.99

Montpellier	FR010C1	29.54	31.038	1.498	0.03	0.96	0.46	0.99
Marseille	FR203C1	30.115	30.696	0.581	0.03	0.94	0.54	0.99
Nice	FR205C2	27.434	33.97	6.536	-1.80	0.98	0.59	0.99
Zagreb	HR001C1	29.878	32.442	2.564	-1.11	0.99	0.62	0.99
Split	HR005C1	28.599	33.525	4.926	-1.72	0.96	0.62	0.99
Budapest	HU001C1	29.493	33.713	4.22	-1.51	0.99	0.84	0.99
Miskolc	HU002C1	29.547	33.466	3.919	-1.54	0.96	0.79	0.99
Pécs	HU004C1	28.859	31.722	2.863	-0.34	0.98	0.48	1.00
Debrecen	HU005C1	28.734	31.762	3.028	-0.07	0.98	0.43	1.00
Szeged	HU006C1	28.664	33.782	5.118	-0.77	0.97	0.70	0.99
Gyõr	HU007C1	30.218	33.047	2.829	-0.97	0.98	0.68	0.99
Dublin	IE001C1	22.212	23.891	1.679	-0.78	0.94	0.86	0.95
Roma	IT001C1	29.169	34.38	5.211	-0.52	0.95	0.74	0.99
Milano	IT002C1	30.059	33.856	3.797	-3.50	1.02	0.99	0.98
Napoli	IT003C1	29.774	34.572	4.798	-0.07	0.92	0.85	0.98
Torino	IT004C1	30.082	32.55	2.467	-3.93	1.02	1.09	0.98
Palermo	IT005C1	27.338	36.016	8.678	-2.23	0.94	0.90	0.98
Genova	IT006C1	26.849	33.256	6.407	-3.04	0.99	0.67	0.99
Bari	IT008C1	27.793	33.836	6.043	-0.70	0.94	0.77	0.99
Bologna	IT009C1	27.771	33.866	6.095	-2.00	1.03	0.71	0.99
Trieste	IT015C1	29.776	32.919	3.143	-1.72	1.00	0.67	0.99
Padova	IT028C1	31.631	34.937	3.307	-2.16	1.02	0.83	0.99
Vilnius	LT001C1	26.119	28.811	2.691	-0.47	0.98	0.59	0.99
Klaipėda	LT501C1	26.463	27.966	1.503	-0.52	0.97	0.55	0.99
Luxembourg	LU001C1	26.843	30.187	3.344	-0.88	0.99	0.52	0.99
Rīga	LV001C1	25.291	26.359	1.068	-0.15	0.97	0.43	1.00
Greater Amsterdam	NL002C2	24.888	28.699	3.812	-0.73	0.96	0.77	0.98
Greater Rotterdam	NL003C2	25.525	29.644	4.118	-0.78	0.96	0.77	0.98

Greater Utrecht	NL004C2	26.183	29.343	3.161	-0.74	0.97	0.80	0.98
Oslo	NO001C1	22.837	23.132	0.294	-2.37	1.05	0.81	0.99
Warszawa	PL001C1	26.733	31.411	4.678	-0.62	0.97	0.58	0.99
Łódź	PL002C1	27.318	30.509	3.192	-0.18	0.97	0.70	0.99
Kraków	PL003C1	24.891	31.403	6.512	-0.94	0.98	0.76	0.99
Wrocław	PL004C1	27.786	32.126	4.34	-0.40	0.98	0.59	0.99
Gdańsk	PL006C1	27.446	29.12	1.675	-0.65	1.00	0.70	0.99
Lisboa	PT001C1	26.688	28.863	2.176	0.22	0.92	0.52	0.98
Porto	PT002C1	28.915	29.236	0.321	-0.25	0.94	0.65	0.98
Bucureşti	RO001C1	29.772	32.411	2.64	-1.51	0.99	0.93	0.99
Cluj-Napoca	RO002C1	25.328	31.889	6.56	-2.32	0.97	1.06	0.99
Braşov	RO504C1	31.309	29.455	-1.854	-2.91	0.99	0.93	0.99
Stockholm	SE001C1	23.409	25.172	1.763	-0.46	0.97	0.57	0.99
Göteborg	SE002C1	24.863	24.815	-0.048	-0.46	0.97	0.57	0.99
Ljubljana	SI001C1	27.059	31.036	3.977	-2.65	1.02	0.84	0.99
Bratislava	SK001C1	29.355	32.998	3.642	-0.90	1.00	0.62	0.99
Košice	SK002C1	29.3	31.49	2.19	-1.41	1.01	0.64	0.99
London Greater City	UK001K1	21.207	28.2	6.993	-0.87	0.99	0.57	0.98
Birmingham	UK002C1	21.682	26.538	4.856	-0.18	0.97	0.74	0.97
Leeds	UK003C1	21.123	25.804	4.682	-1.09	0.93	0.78	0.96
Glasgow	UK004C1	21.676	24.349	2.673	-1.16	0.96	0.82	0.96
Edinburgh	UK007C1	21.133	24.516	3.383	-0.45	0.95	0.75	0.97
Newcastle upon Tyne	UK013C1	21.031	23.787	2.757	-1.84	0.99	0.73	0.98

Supplement E. Counterfactual scenarios.

a) *Urban Heat Island (UHI)*

We retrieved the mean day-time UHI and mean night-time UHI data at 100 m x 100 m resolution for 2015 summer season (ie, June - August) from the Copernicus UrbClim model application. This is the difference between the mean rural temperature (ie, represented by the rural classes of CORINE covering grassland, cropland, shrubland, woodland, broadleaf forest and needleleaf forest) and each of the urban grid cells, masking out the water bodies (13).

We estimated the 250m grid cell mean 24hs UHI (ie, for each day) by averaging the day and night UHI 100 m grid cells with centroids within the spatial boundaries of each 250 m grid cell. For the grids with negative values we considered a null UHI. We have also calculated the average daytime and night-time UHI separately to understand the contribution of each to the mean 24hs UHI. Day-time UHI resulted in a mean city value of 0.6ºC, whereas night-time UHI was 1.9ºC.

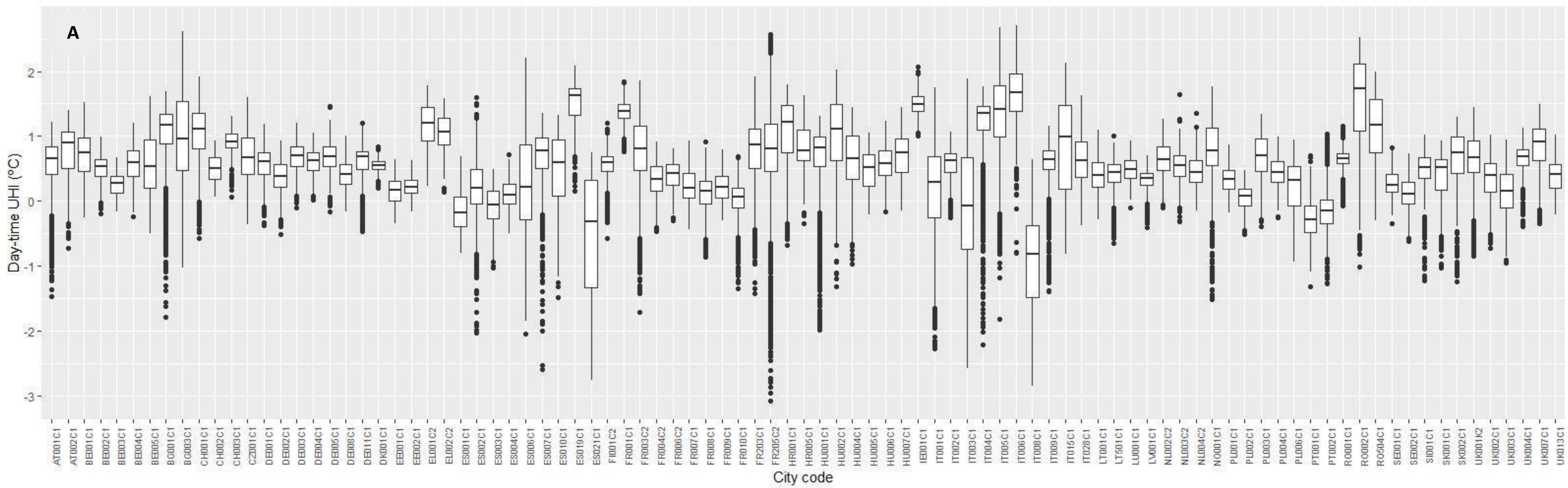

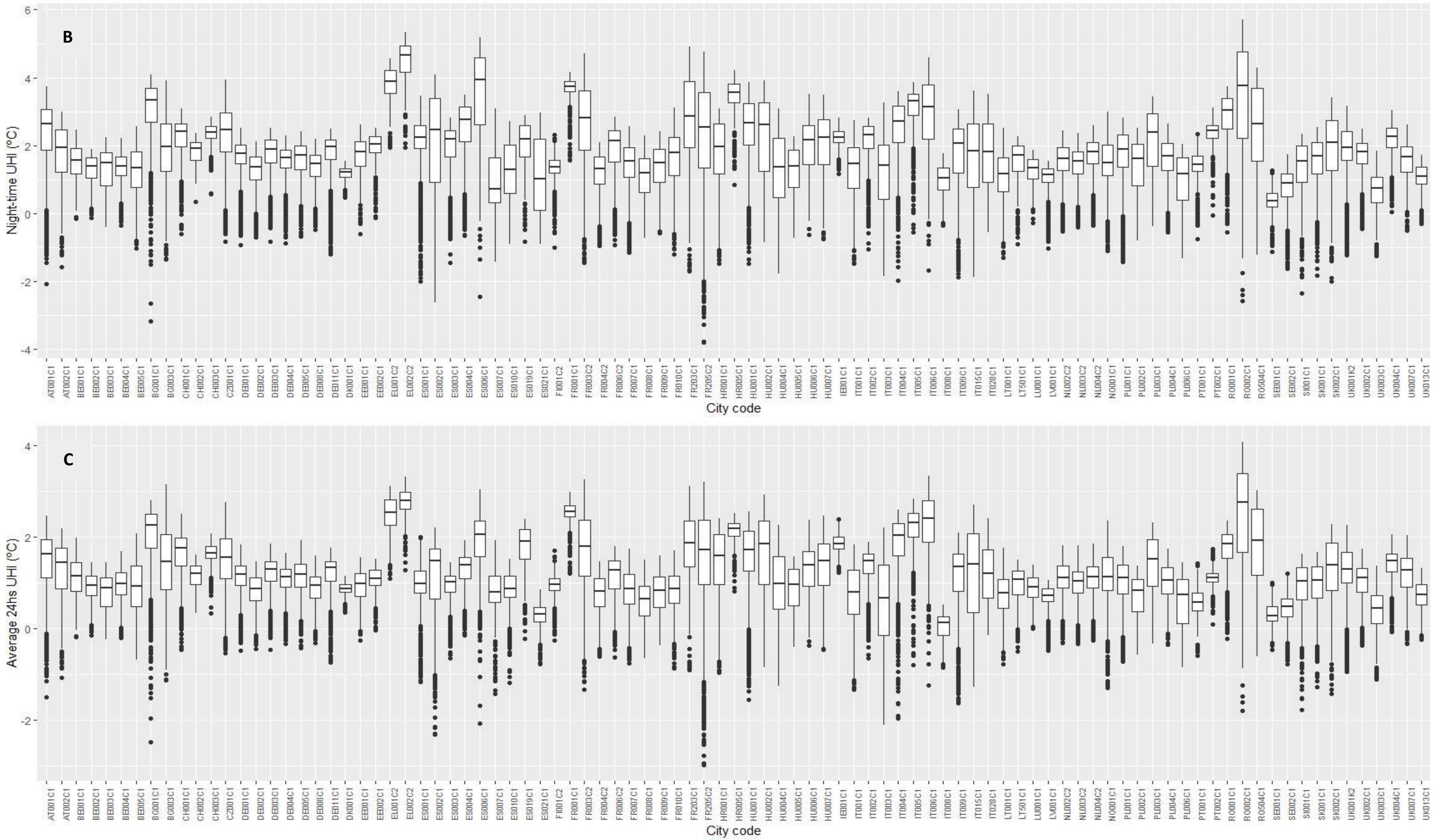

Figure S5. (A) *Day-time average urban heat island per grid cell.* ***(B).*** *Night-time average urban heat island per grid cell.* ***(C)*** *24 hours average urban heat island per grid cell.*

Table S4. *Distribution of the percentage of negative daily UHI values for day-time (UHId) and night-time (UHIn)*

	Minimum (%)	Pct.[1] 25 (%)	Median (%)	Mean (%)	Pct.[1] 75 (%)	Maximum
UHId	0.00	5.94	11.67	17.96	23.49	80.07
UHIn	0.00	1.10	3.61	5.07	7.88	22.67

[1]. Pct.=percentile

We also estimated the population-weighted city-average by weighting the number of people in a city—divided by the grid—to the UHI exposure in each grid-cell. By summing up all grid-cells estimations, it is possible to have a more accurate measure of the exposure of the city population as it gives proportionately greater weight to the UHI exposure where most people live.

b) TC 30%

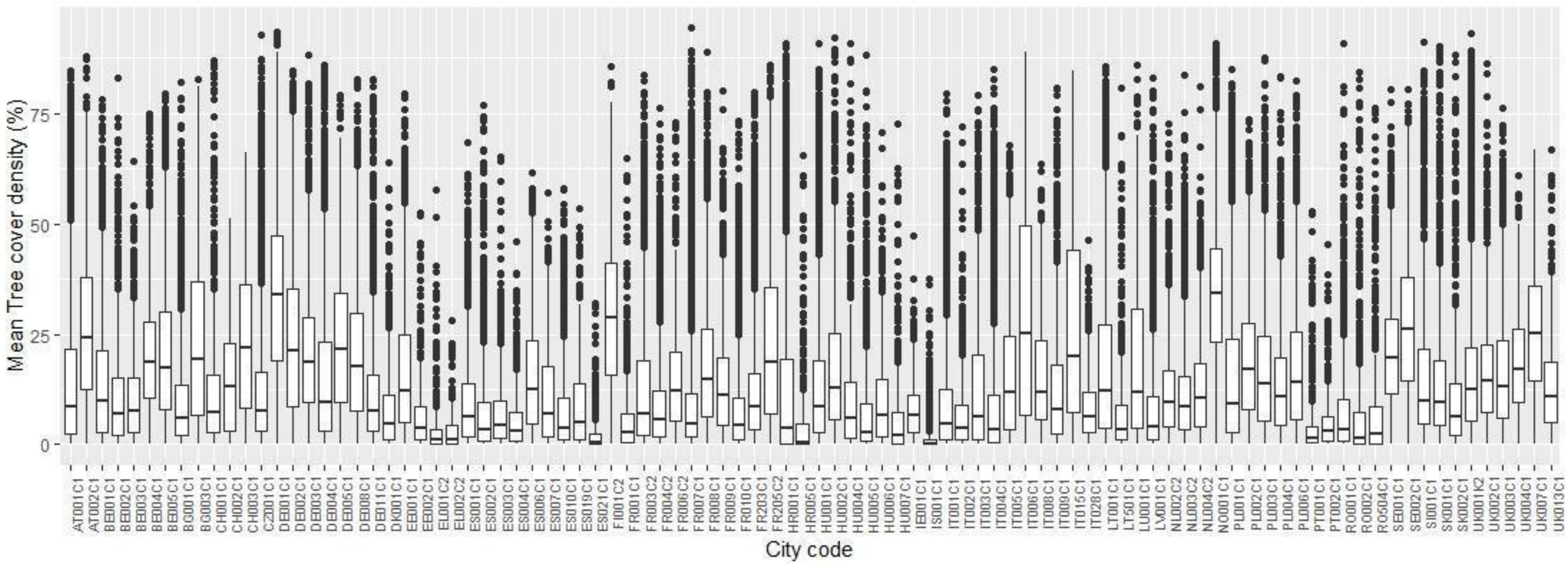

Figure S6. *Average tree cover density at a grid cell level by city.*

For each city, we analyzed the feasibility of achieving the 30% TC target. We estimated the percentage of open space in each city at a grid cell level where potentially trees could be planted according to the corresponding land use. For this purpose, we retrieved from the European Settlement Map (ESM) the open space (“BU area -open space”) and the green space (“BU - green NDVIx”; green spaces not included in the Urban Atlas (UA) green space classification, such as roadside vegetation, urban trees and pocket parks). We estimated the difference between the 30% target and the available open space at a grid cell level (Figue S7). We calculated the mean and the interquartile range at a city level in order to have the whole picture of the open space distribution (Table S5).

Table S5. *Interquartile range of the difference between the 30% TC target and the open space by grid-cell.*

City code	Quartile 1	Median	Quartile 3	Mean	City code	Quartile 1	Median	Quartile 3	Mean
AT001C1	0.00	0.00	0.00	2.09	HU001C1	0.00	0.00	0.00	0.91
AT002C1	0.00	0.00	0.00	1.65	HU002C1	0.00	0.00	0.00	2.24
BE001C1	0.00	0.00	12.33	6.18	HU004C1	0.00	0.00	0.00	1.30
BE002C1	0.00	0.00	0.23	2.24	HU005C1	0.00	0.00	0.00	1.80
BE003C1	0.00	0.00	0.85	2.48	HU006C1	0.00	0.00	0.00	1.90
BE004C1	0.00	0.00	0.00	0.52	HU007C1	0.00	0.00	0.94	2.82
BE005C1	0.00	0.00	0.00	1.11	IE001C1	0.00	0.00	0.00	0.12
BG001C1	0.00	0.00	0.00	0.47	IT001C1	0.00	0.00	0.00	1.03
BG003C1	0.00	0.00	0.00	1.07	IT002C1	0.00	0.00	0.00	1.71
CH001C1	0.00	0.00	2.54	2.73	IT003C1	0.00	0.00	0.00	1.05
CH002C1	0.00	0.00	6.23	3.50	IT004C1	0.00	0.00	0.00	1.11
CH003C1	0.00	0.00	5.84	3.68	IT005C1	0.00	0.00	0.00	1.02
CZ001C1	0.00	0.00	0.00	1.37	IT006C1	0.00	0.00	0.00	1.92
DE001C1	0.00	0.00	0.00	1.99	IT008C1	0.00	0.00	0.00	0.95
DE002C1	0.00	0.00	0.00	2.40	IT009C1	0.00	0.00	0.00	1.95
DE003C1	0.00	0.00	0.00	0.71	IT015C1	0.00	0.00	0.00	1.92
DE004C1	0.00	0.00	0.00	1.47	IT028C1	0.00	0.00	0.00	0.53
DE005C1	0.00	0.00	5.91	3.45	LT001C1	0.00	0.00	0.00	1.58
DE008C1	0.00	0.00	0.00	0.76	LT501C1	0.00	0.00	0.00	1.14
DE011C1	0.00	0.00	0.00	1.56	LU001C1	0.00	0.00	1.95	2.74
DK001C1	0.00	2.35	13.48	6.75	LV001C1	0.00	0.00	0.00	1.19
EE001C1	0.00	0.00	0.00	0.41	NL002C2	0.00	0.00	3.53	3.18
EE002C1	0.00	0.00	0.00	0.67	NL003C2	0.00	0.00	5.00	3.33
EL001C2	0.00	0.00	1.69	1.24	NL004C2	0.00	0.00	6.54	3.97
EL002C2	0.00	0.00	0.00	0.35	NO001C1	0.00	0.00	0.00	1.73
ES001C1	0.00	0.00	0.00	1.65	PL001C1	0.00	0.00	0.00	1.02
ES002C1	0.00	0.00	10.46	5.37	PL002C1	0.00	0.00	0.00	1.95

ES003C1	0.00	0.00	0.00	1.98	PL003C1	0.00	0.00	0.00	1.65
ES004C1	0.00	0.00	4.49	3.47	PL004C1	0.00	0.00	0.00	2.16
ES006C1	0.00	0.00	3.18	3.56	PL006C1	0.00	0.00	0.00	1.06
ES007C1	0.00	0.00	0.00	1.47	PT001C1	0.00	0.00	6.46	3.70
ES010C1	0.00	0.00	0.20	2.22	PT002C1	0.00	0.00	0.66	2.05
ES019C1	0.00	0.00	11.06	5.78	RO001C1	0.00	0.00	0.00	1.33
ES021C1	0.00	0.00	0.27	3.46	RO002C1	0.00	0.00	3.42	3.02
FI001C2	0.00	0.00	0.00	0.19	RO504C1	0.00	0.00	4.27	3.98
FR001C1	0.00	6.84	13.01	7.50	SE001C1	0.00	0.00	0.00	1.78
FR003C2	0.00	0.00	0.00	1.62	SE002C1	0.00	0.00	4.12	3.26
FR004C2	0.00	0.00	0.00	1.88	SI001C1	0.00	0.00	5.96	4.17
FR006C2	0.00	0.00	0.00	1.71	SK001C1	0.00	0.00	3.10	2.89
FR007C1	0.00	0.00	0.00	1.55	SK002C1	0.00	0.00	5.46	3.73
FR008C1	0.00	0.00	6.38	3.83	UK001K2	0.00	0.00	0.00	2.85
FR009C1	0.00	0.00	0.56	2.29	UK002C1	0.00	0.00	0.00	1.09
FR010C1	0.00	0.00	3.40	3.20	UK003C1	0.00	0.00	4.94	4.45
FR203C1	0.00	0.00	0.00	2.27	UK004C1	0.00	0.00	0.62	2.78
FR205C2	0.00	0.00	0.00	2.63	UK007C1	0.00	0.00	15.00	7.66
HR001C1	0.00	0.00	0.00	1.90	UK013C1	0.00	0.00	0.00	2.48
HR005C1	0.00	0.00	0.00	0.52					

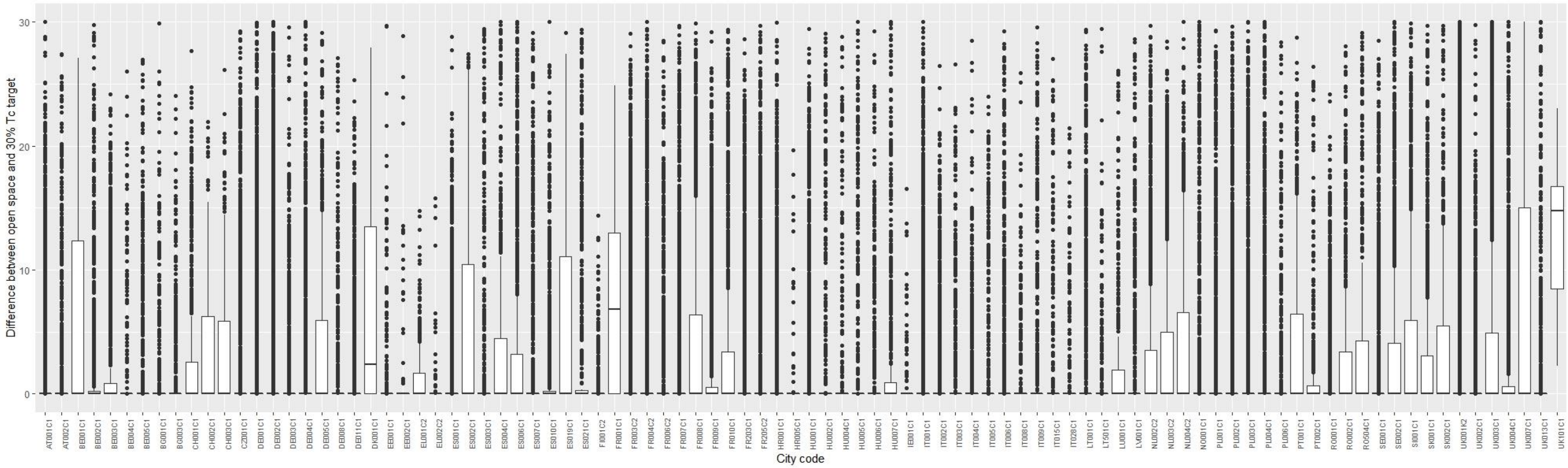

Figure S7. *Difference between 30% target and the open space at a grid cell level for each city.*

Table S6. *Statistical distribution of Equation 2 coefficients and determinant coefficient (R^2)*

β_{0e4}	β_{1e4}	β_{2e4}	R^2
36.42 ± 5.50	-0.06 ± 0.003	-1.49 ± 1.01	0.41 ± 0.20

Eq. 2 was built with an US air temperature dataset given that the existing network of weather stations in Europe has insufficient coverage. The dataset, compiled by the University of Colorado Denver, derived from NOAA (National Oceanic and Atmospheric Administration), consists of more than 6,500 summer maximum air temperature records (June 15th to August 15th) from weather stations, including their latitude and the average of 1 km of neighbourhood LST buffer of each station. The wide range of latitudes and biomes covered makes the associations suitable for extrapolation to Europe.

In order to test the model predictions, we used average summer (June–August 2015) air temperature at a city level to validate the air temperature estimated through the model. With this purpose we regressed each city-average value against the corresponding observed air temperature values. We calculated the adjusted R2, RMSE and model coefficients to assess the accuracy of the model.

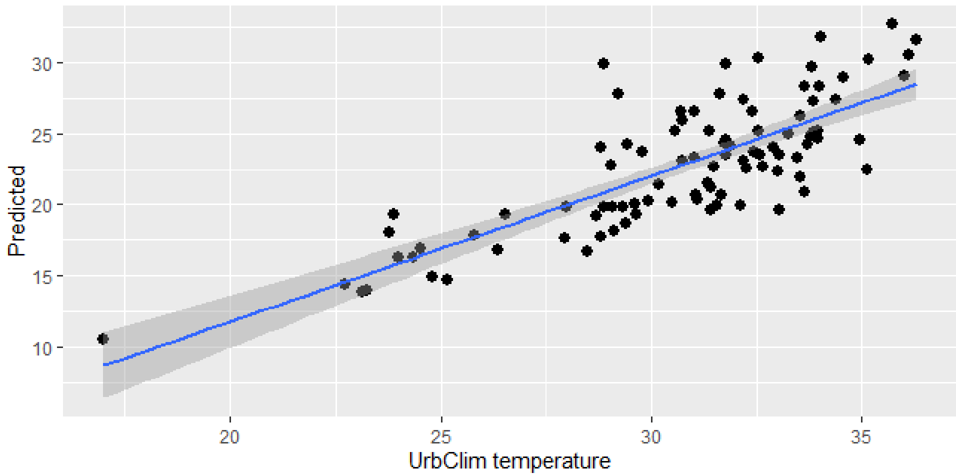

Figure S8. *Plot of the cooling model validation. The UrbClim temperature data used in the validation is the average maximum temperature from June to August 2015. Adjusted R2: 0.66; RMSE: 2.03. Both intercept and slope are significant for p ≤ 0.05.*

In order to estimate the LST corresponding to TC equal to 30%, 40% and 25%, we estimated the city-average Etree considering the grid cells with: (1) TC=28-32% (Etree30) and, (2) TC=38-44% (Etree40), (3) TC=23-27% (Etree25), respectively. We considered an interval plus-minus 2º for avoiding NAs or low counts.

For two cities (ie, Thessaloniki, Greece and Murcia, Spain) for which the maximum TC was 30% we computed the same mean evapotranspiration for TC=40%.

Table S7. *Distribution of the percentage of negative cooling estimations for TC=30%*

	Minimum (%)	Pct.[1] 25 (%)	Median (%)	Mean (%)	Pct.[1] 75 (%)	Maximum (%)
Cooling (TC=30%)	0.1	6.63	14.04	16.36	21.82	89.4

[1]. Pct.=percentile

Model errors

We estimated the uncertainty of the model by calculating the propagated error of the two regressions, for each city. We applied Eq. S1 based on Taylor el al method for accumulated prediction fractional uncertainties (14).

(Eq. S4) $$\text{Error} = \sqrt{(\delta Ta / |Ta|)^2 + (\delta LST / |LST|)^2 + (\delta Ta_{30} / |Ta_{30}|)^2 + (\delta LST_{30} / |LST_{30}|)^2}$$

Where δ is the error, Ta is the estimated air temperature, LST is the land surface temperature, and Ta_{30} and LST_{30} are the estimated air and surface temperature for TC=30% scenario, respectively. We calculated the errors (δ) by averaging the observed upper and lower confidence interval (alpha = 0.05) values from grid- cell-level predictions,

Supplementary F. Sensitivity analysis.

a) Health impact assessment of urban heat island

i) Exposure response function (Martinez-Solanas et al, 2021)

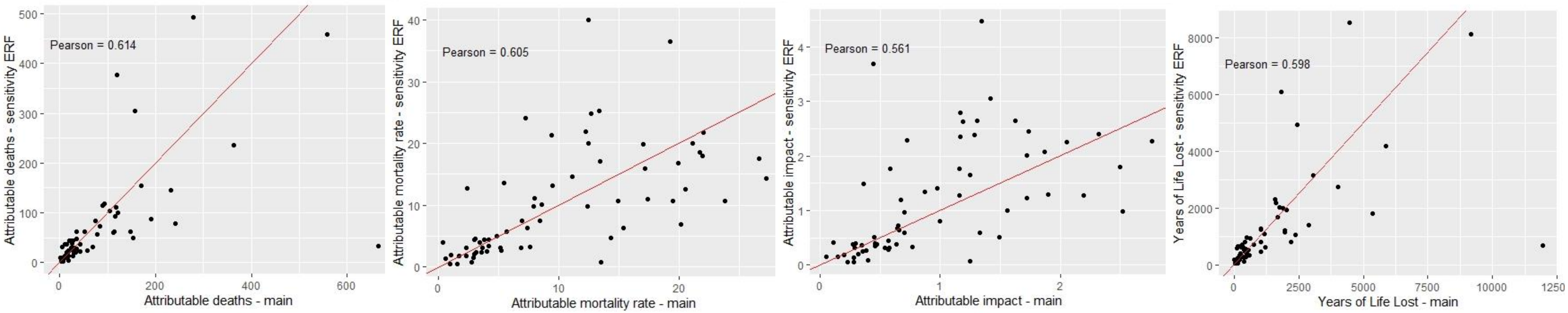

ii) Grid-cell-average summer UHI

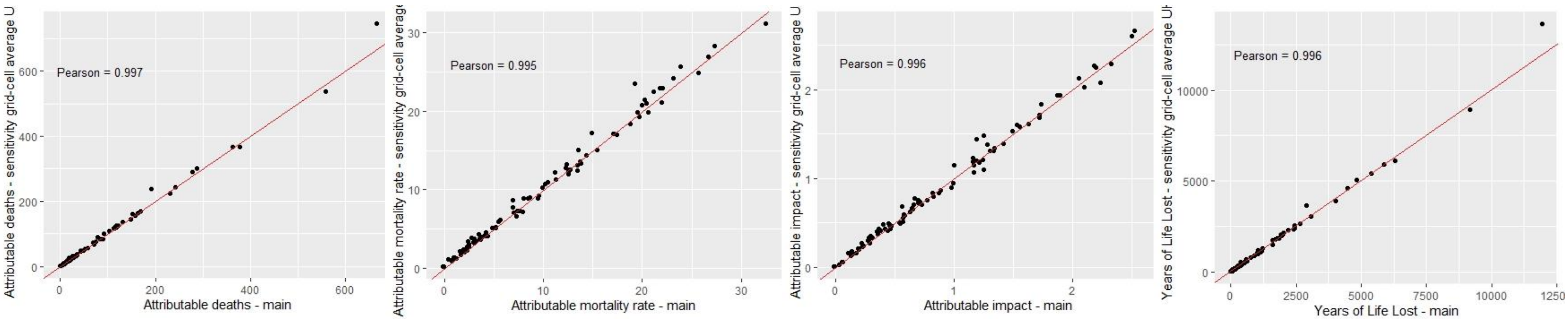

iii) City-average UHI

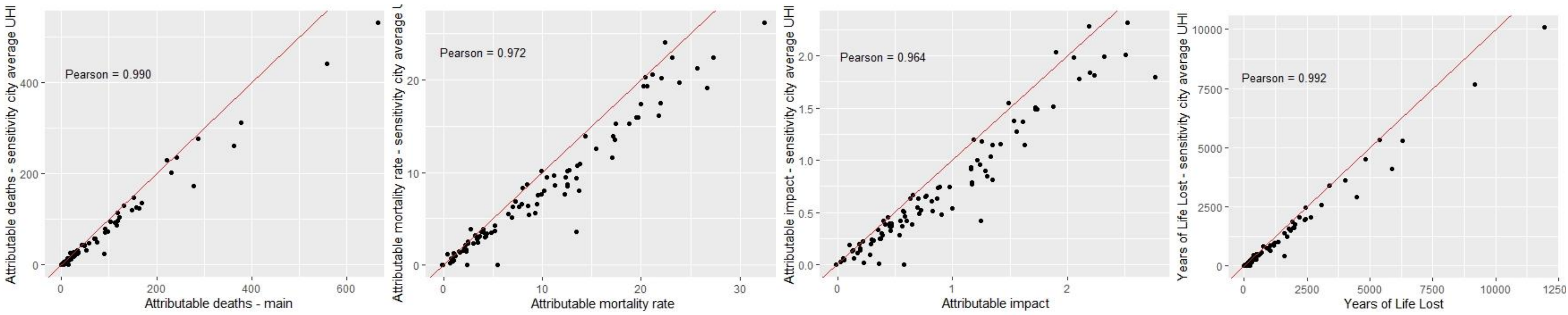

iv) Adjusted annual city mortality dataset

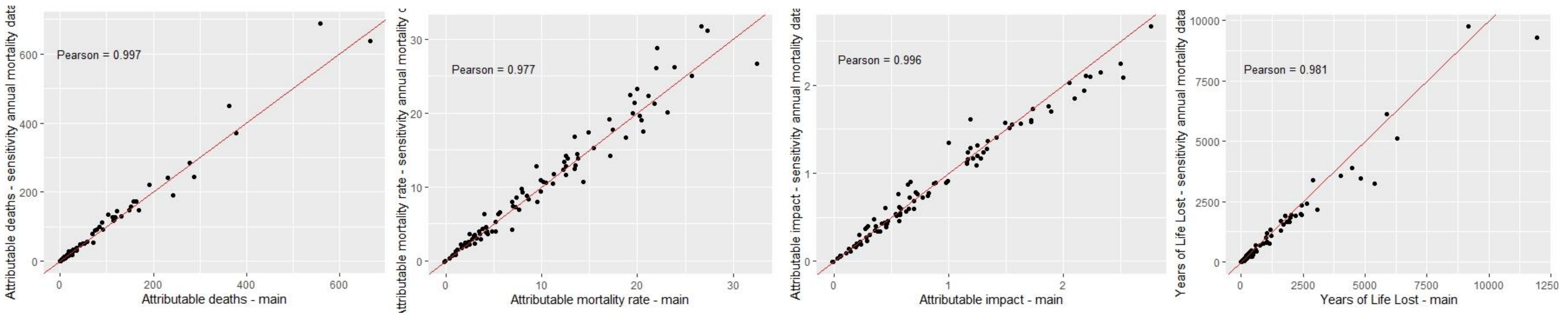

v) Non-adjusted annual city mortality dataset

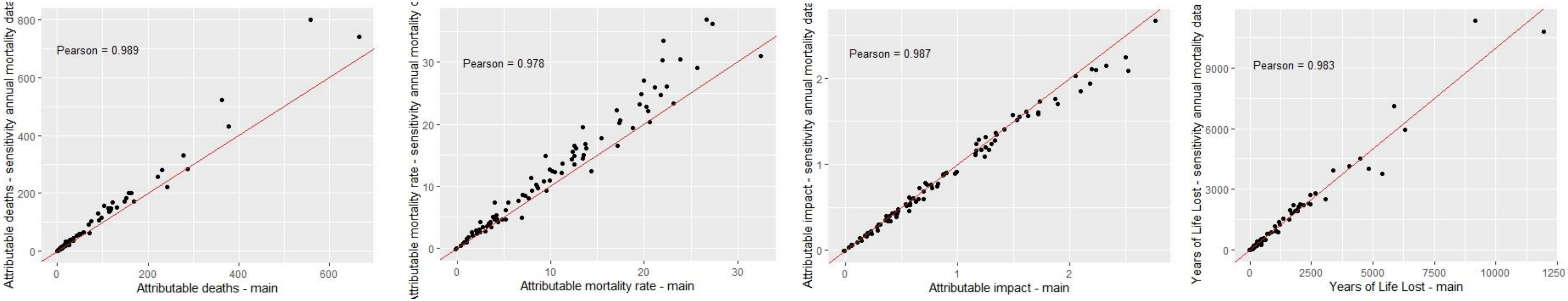

b) Cooling estimation

We conducted two sensitivity analysis of the cooling estimation for TC=30% changing the way the amount of water evaporated from trees (E_{tree30}) was calculated.

1) Linear regressions by city between the TC and E_{tree}

2) Linear regression by biome between the TC and E_{tree}

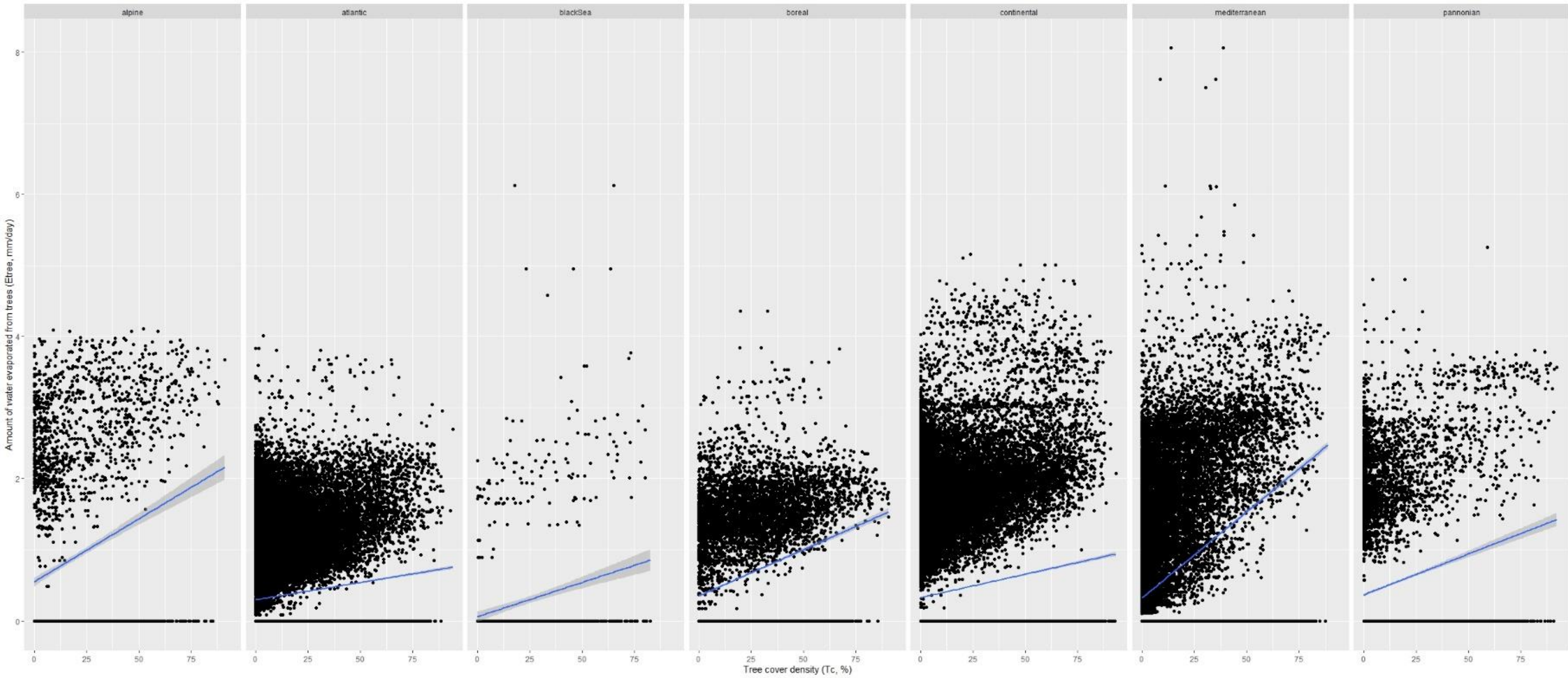

c) 30% TC health impact assessment

i) $Etree_{30}$ estimation: regression by city

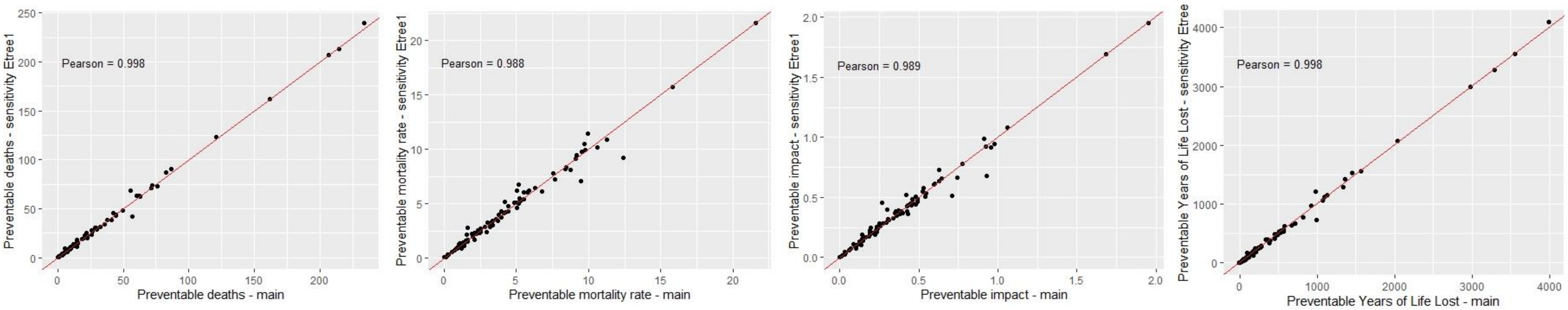

ii) $Etree_{30}$ estimation: linear regression by biome

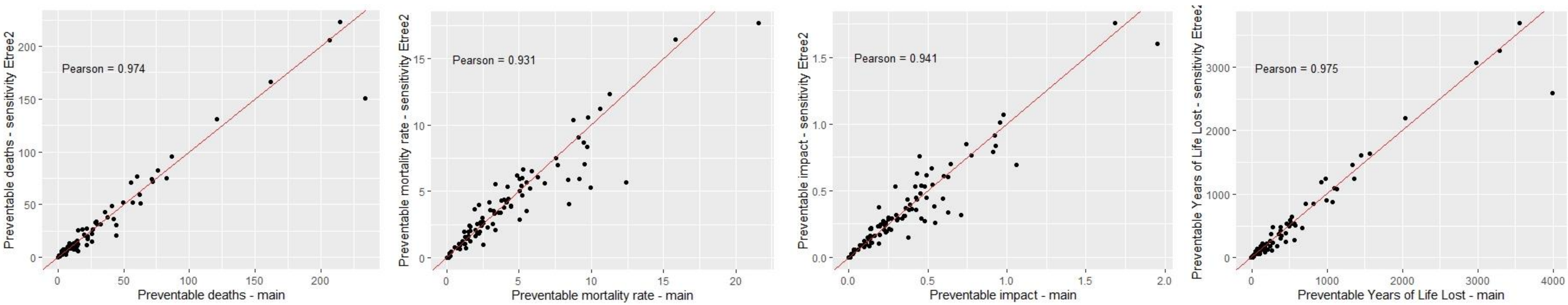

iii) City-average cooling

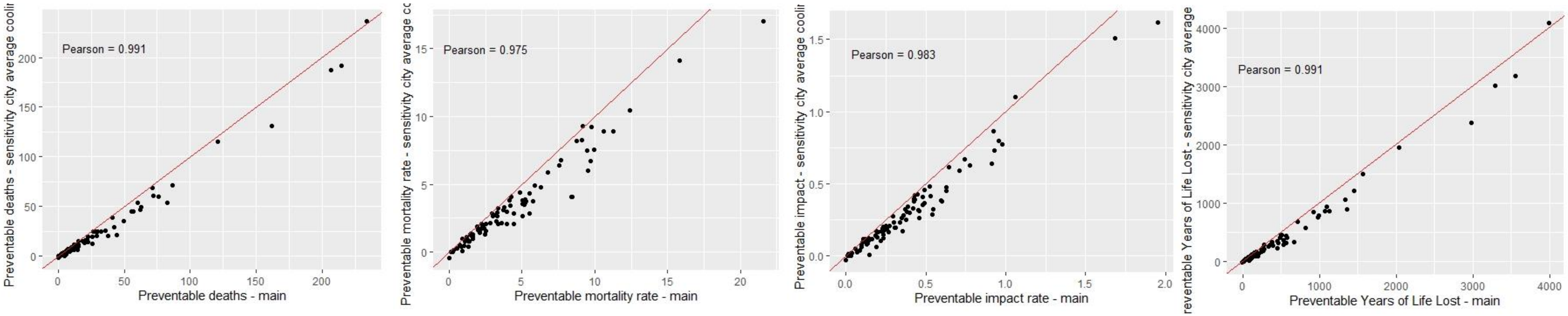

iv) Exposure response function (Martinez-Solanas et al, 2021)

We applied the same methodology than for the main analysis.

Given that the risk estimates were built under the E-obs dataset (15), we applied a city-specific correction to the UrbClim dataset as:

Eq. (S5) $T_{urbclim} = \alpha + \beta 3 * T_{E\text{-}obs}$

Where $T_{urbclim}$ is the mean UrbClim daily city-level temperature and $T_{E\text{-}obs}$ is the mean E-obs daily city-level temperature for 2015.

After adjusting the temperature dataset, there were still some days with temperature values falling out of the ERFs (ie, temperature values above the maximum temperature with an estimated risk). We chose a conservative approach and instead of extrapolating the ERFs above the maximum, we assigned to highest temperatures, the corresponding maximum temperature´ risk available.

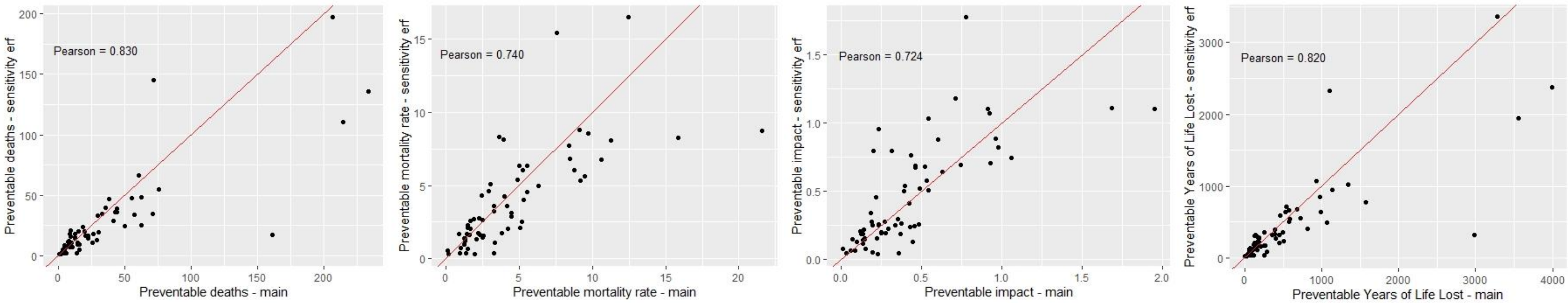

Supplementary analysis G. Uncertainty analyses.

We conducted uncertainty analysis running 500 Monte Carlo simulations considering each of the parameter's uncertainty separately. We considered the following sources of uncertainties: the ERFs (8), the UrbClim data error (16), the temperature adjustment model error, the UHI data error (16) and the cooling model error, accordingly.

- ***Urban heat island health impact assessment***

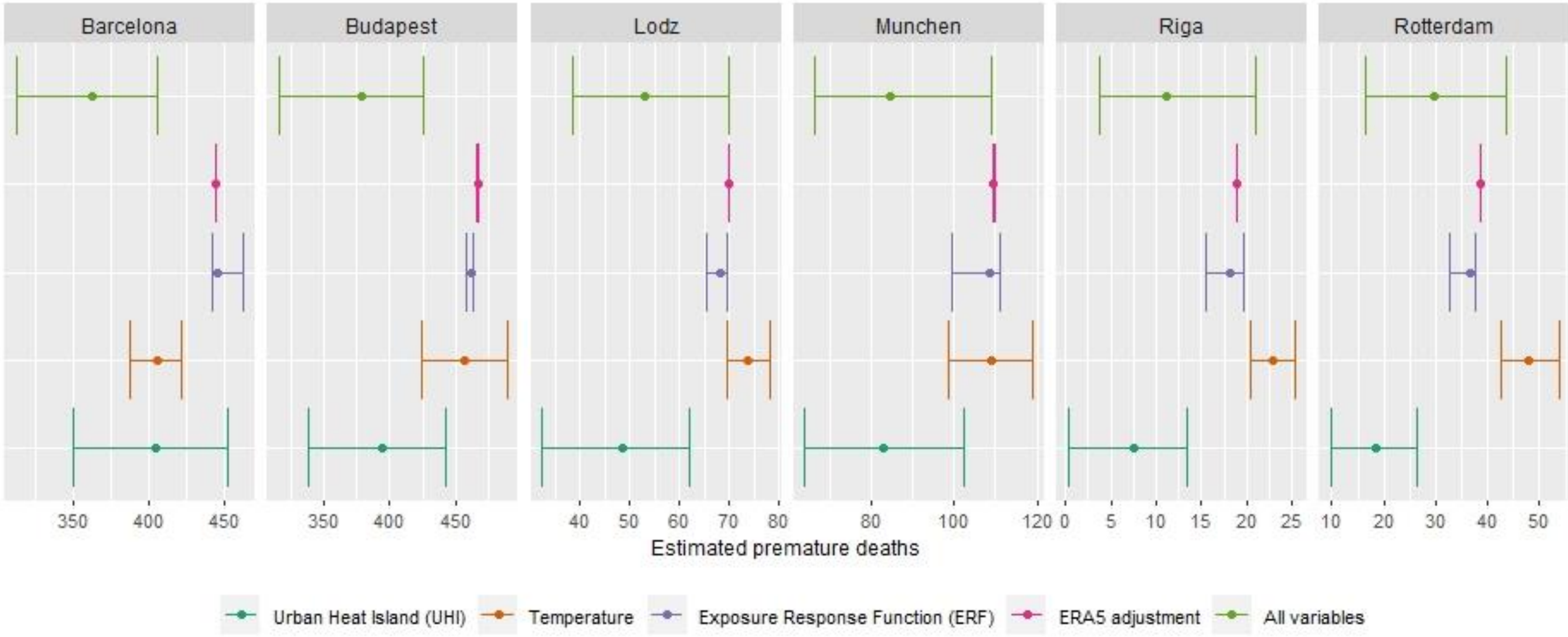

- ***30% TC scenario health impact assessment***

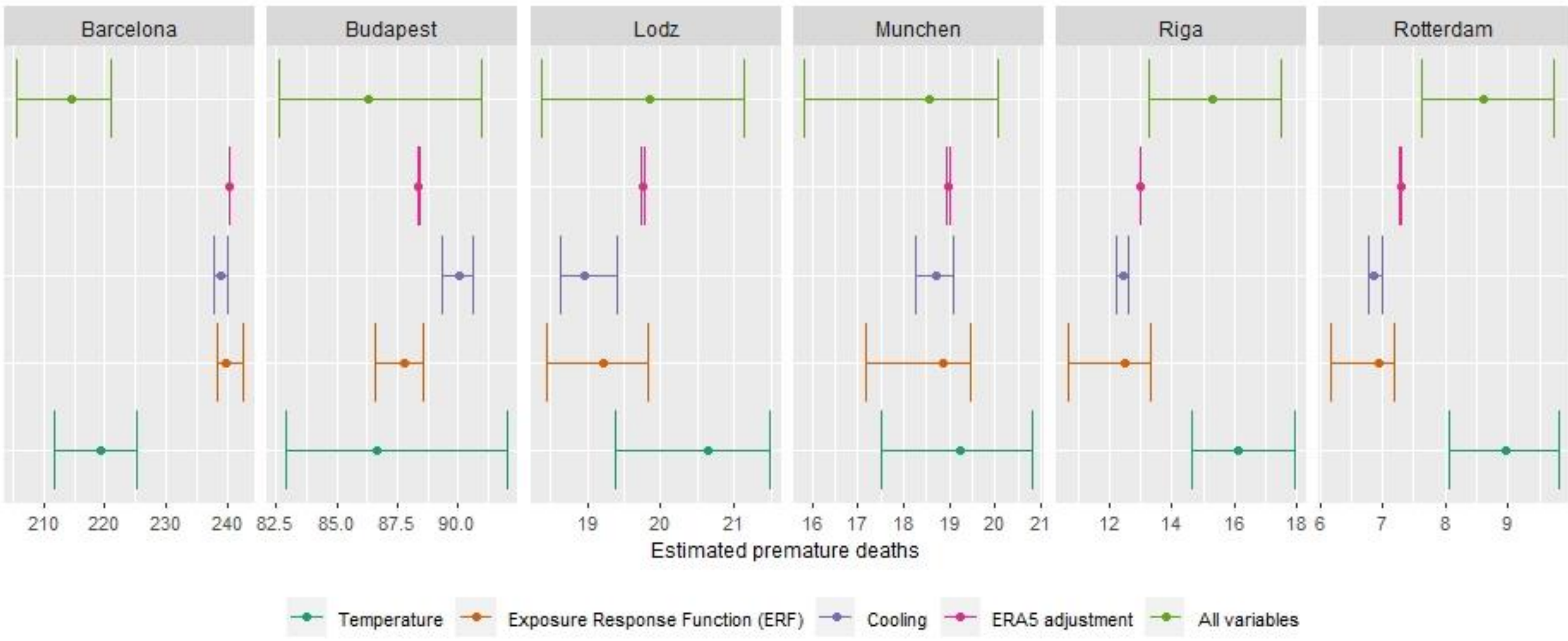

References

1. Eurostat. Urban Audit. 2018; Available from: https://ec.europa.eu/eurostat/web/cities/data/database
2. Dijkstra, L. & Poelman H. Cities in Europe. The new OECD-EC definition. 2012;
3. European Commission. Global Human Settlement [Internet]. 2019 [cited 2021 Sep 14]. Available from: https://ghsl.jrc.ec.europa.eu/data.php
4. Copernicus. Urban Atlas 2012. 2012.
5. Eurostat. Regional statistics by NUTS classification. 2019.
6. Eurostat. NUTS - NOMENCLATURE OF TERRITORIAL UNITS FOR STATISTICS. 2018.
7. Eurostat. Database [Internet]. [cited 2021 Dec 27]. Available from: https://ec.europa.eu/eurostat/data/database
8. Masselot P. Excess mortality attributed to heat and cold in 801 cities in Europe. Forthcoming.
9. Lee W, Kim H, Hwang S, Zanobetti A, Schwartz JD, Chung Y. Monte Carlo simulation-based estimation for the minimum mortality temperature in temperature-mortality association study. BMC Med Res Methodol. 2017;17(1):1–10.
10. Eurostat. Revision of the European Standard Population. Report of Eurostat's task force. 2013.
11. Eurostat. Life expectancy at birth by sex [Internet]. [cited 2021 Nov 10]. Available from: https://ec.europa.eu/eurostat/databrowser/view/tps00205/default/table?lang=en
12. WHO. WHO methods and data sources for global burden of disease estimates 2000-2011. 2013;(November):86. Available from: http://www.who.int/healthinfo/statistics/GlobalDALYmethods_2000_2011.pdf?ua=1
13. Copernicus. Corine Land Cover [Internet]. 2012 [cited 2021 Sep 3]. Available from: https://land.copernicus.eu/pan-european/corine-land-cover
14. Taylor J. Introduction to Error Analysis, the Study of Uncertainties in Physical Measurements, 2nd Edition. 1997.
15. European Climate Assessment & Dataset project. E-OBS gridded dataset [Internet]. [cited 2021 Nov 15]. Available from: https://www.ecad.eu/download/ensembles/download.php
16. De Ridder K, Lauwaet D, Maiheu B. UrbClim – A fast urban boundary layer climate model. Urban Clim [Internet]. 2015 Jun 1 [cited 2020 Mar

19];12:21–48. Available from: https://www.sciencedirect.com/science/article/abs/pii/S2212095515000024?via%3Dihub